The Astronomical Journal, 157:228 (19pp), 2019 June https://doi.org/10.3847/1538-3881/ab18a9

Light Curves and Rotational Properties of the Pristine Cold Classical Kuiper Belt Objects

Audrey Thirouin[1] and Scott S. Sheppard[2]
[1] Lowell Observatory, 1400 W. Mars Hill Road, Flagstaff, AZ, 86001, USA; thirouin@lowell.edu
[2] Department of Terrestrial Magnetism (DTM), Carnegie Institution for Science, 5241 Broad Branch Road NW, Washington, DC, 20015, USA
Received 2019 January 24; revised 2019 March 13; accepted 2019 April 3; published 2019 May 14

Abstract

We present a survey of the rotational and physical properties of the dynamically low inclination Cold Classical (CC) trans-Neptunian objects (TNOs). The CCs are primordial planetesimals and contain information about our solar system and planet formation over the first 100 million years after the Sun's formation. We obtained partial/complete light curves for 42 CCs. We use statistical tests to derive general properties about the shape and rotational frequency distributions of the CCs and infer that they have slower rotations and are more elongated/deformed than the other TNOs. On the basis of the full light curves, the mean rotational period of the CCs is 9.48 ± 1.53 hr compared to 8.45 ± 0.58 hr for the rest of the TNOs. About 65% of the TNOs have a light-curve amplitude below 0.2 mag compared to the 36% of CCs with small amplitude. We present the full light curve of one likely contact binary, 2004 VC_{131}, with a potential density of 1 g cm^{-3} for a mass ratio of 0.4. We have hints that 2004 MU_8 and 2004 VU_{75} are perhaps potential contact binaries, on the basis of their sparse light curves, but more data are needed to confirm this finding. Assuming equal-sized binaries, we find that ∼10%–25% of the CCs could be contact binaries, suggesting a deficit of contact binaries in this population compared to previous estimates and to the (∼40%–50%) possible contact binaries in the Plutino population. These estimates are lower limits and may increase if nonequal-sized contact binaries are considered. Finally, we put in context the results of the *New Horizons* flyby of 2014 MU_{69}.

Key words: Kuiper belt objects: individual (2004 VC_{131}, 2004 MU_8, 2004 VU_{75}) – techniques: photometric

Supporting material: figure set, machine-readable tables

1. Dynamically Cold Classical (CC) Trans-Neptunian Objects (TNOs)

In this study, we target the dynamically CC TNOs, one of the trans-Neptunian subpopulations. The CCs with semimajor axes from ∼40 up to ∼48 au have low inclinations and low eccentricities ($e < 0.24$) (Gladman et al. 2008). Generally, in the case of the inclination, the cutoff is at 4°–5°. However, according to surface colors analysis, a limit at ∼12° seems more appropriate (Peixinho et al. 2008).

Among the entire trans-Neptunian belt, the CCs are the least evolved TNOs (Batygin et al. 2011). Over the years, it has been argued that the CCs have likely been formed in situ and, thus, have remained far from the Sun, and have never undergone any catastrophic dynamical evolution. For all of these reasons, the CCs are pristine planetesimals and, therefore, have important indications about the early age of our solar system regarding composition, rotational properties, dynamics, accretion, and collisional theories.

The CC population displays several properties that make them stand out compared to the other TNO populations. Their surfaces are very-red/ultra-red, and according to a recent photometric survey, the CCs are also distinguishable in the *z*-band (Benecchi et al. 2009; Pike et al. 2017). Another characteristic feature of the CC population is the large amount of resolved equal-sized wide binaries. Thanks to extensive surveys with the *Hubble Space Telescope* (*HST*), Noll et al. (2008a, 2014) inferred that all the large CCs with $H \geqslant 6$ mag are equal-sized wide binaries. In the entire CC population, the fraction of resolved binaries is 22^{+10}_{-5}% compared to the 5.5^{+4}_{-2}% in the other dynamical populations (Stephens & Noll 2006). Because most of the CCs are likely primordial, their rotational properties are likely primordial too, but care has to be taken with the binary systems, as tidal effect(s) can affect their rotations.

The *NASA*'s New Horizons spacecraft flew by a small CC in 2019 January named (486958) 2014 MU_{69} (Stern et al. 2019). Therefore, it is crucial to have context for the flyby results, and the best way for this purpose is to study a large sample of CCs and derive as much information as possible. Also, on the basis of a multichords stellar occultation (and confirmed by the flyby), 2014 MU_{69} is a contact binary, so it is useful to find more of them for comparison and understand their formation/evolution as well as constrain their fraction across the trans-Neptunian belt (Moore et al. 2018).

We present here a survey dedicated to the rotational features of the CC population. In the following sections, we will present our survey (Section 2), as well as our sparse/complete light curves of 42 CCs (Section 3). In Section 4, we will derive information about the shape and rotational frequency distribution of the CC population. We will also compare the contact binary fraction of the CCs and the Plutinos, as well as the main rotational properties of the CCs and the rest of the TNOs (Section 5). Also, we will provide some context for the second flyby of the *NASA New Horizons* mission (Section 6). Finally, we will summarize our findings.

2. Survey Design, Observational Facilities, and Data

We carried out a survey dedicated to the CCs with the 6.5 m Magellan-Baade Telescope and the Lowell Observatory's 4.3 m Discovery Channel Telescope (DCT). So far, we compiled a sample of 42 partial/complete rotational light curves for CCs with absolute magnitudes from 5 to 7.2 mag

(Tables 1 and 2). In Figure 1, all known TNOs with a semimajor axis from 38 to 50 au, an inclination up to 20°, and an eccentricity up to 0.4 are plotted. Objects reported in this work are highlighted with different colors and symbols (see Section 4 for more details). Our targets have an inclination $i \leqslant 5°$ (the cutoff generally used to distinguish Hot from CCs), except 2004 OQ_{15}, which has an inclination of 9.°7, and 2014 GZ_{53}, with $i = 5.°9$.

We aim to identify the primordial characteristic(s) of this population compared to the rest of the TNOs. We also want to test different size regimes, pushing toward smaller objects as they are underrepresented in the literature, as well as the discovery of potential contact binaries also lacking in the literature. In majority, the resolved binary CCs have been studied in the past and, thus, we are focusing on the single objects and nonresolved binaries (i.e., contact/close binaries).

Our survey is designed to test the short- and long-term variability of the CC population. In fact, according to Sheppard et al. (2008), Duffard et al. (2009), Thirouin et al. (2010, 2014), and Benecchi & Sheppard (2013), TNOs have a mean periodicity of about 8 hr, but binary/multiple systems have the tendency to rotate slower than the single objects. Therefore, it is crucial to test a potential variability over a couple of hours (i.e., the short-term variability) and variability over several days (i.e., the long-term variability). Thus, when we observe a TNO for sparse light curve, we ideally want to observe it over a night and reobserve it a couple of days up to month after the first run. With such a strategy, we can evaluate the likelihood of a short and/or long rotational period. This strategy highly depends on the observing schedule and the weather conditions, thus, on some occasions, we can test only the short-term variability.

Our survey strategy is to observe a large sample of CCs for partial light curves, which allow us to constrain the rotational period and the variability. These light curves are crucial to identifying interesting targets with a large amplitude, typically >0.4 mag, but also are crucial once we have to calculate the contact binary fraction, the fraction of spherical or elongated objects, and thus have a distribution of shapes for the CC population. If an object is showing a large amplitude (>0.4 mag) over a few hours or days, we will attempt to get its full light curve, but if an object is not showing a significant variability (<0.2 mag), we will not obtain its full light curve. For objects with a moderate amplitude (around 0.3 mag), we will also schedule them for full light curve, but they have a lower priority than the large-amplitude objects and, thus, may not be reobserved on the basis of the amount of observing time available to us. Our cutoff at 0.4 mag allows us to favor objects with an elongated shape and potential contact binaries, which are our highest priorities. With such a strategy, we may miss some very slow rotators with a large amplitude, and to avoid this we try to reobserve our targets a couple of days/months after the first observations (if the observing schedule and weather allow us to do so). Unfortunately, slow rotators (with large or small amplitude) are difficult to detect for the ground, mainly because of the large amount of observing time needed, as well as the 24 hr aliasing effect. Therefore, our survey and all other ground-based surveys are biased against slow rotators. So far, the rotational periods of the likely/confirmed contact binaries are between ∼6 and ∼16 hr, with the exception of one with a period of ∼35 hr (Thirouin & Sheppard 2018). Because we are trying to have at least an observing block of about 5 hr per object, we are able to cover a reasonable amount of the object's rotation and thus identify any object of interest. In the case of 2014 JL_{80}, with a period of about 35 hr, two nights were needed to confirm the large amplitude. The fact that our team was able to identify 2014 JL_{80} as an object of interest demonstrates that our strategy is adequate for our purpose (Thirouin & Sheppard 2018).

Our two main facilities are the Magellan-Baade telescope and the Lowell's DCT. At Las Campanas Observatory (Chile), the 6.5 m Magellan-Baade telescope is equipped with IMACS (Inamori-Magellan Areal Camera & Spectrograph). This instrument is a wide-field imager with a 27.′4 diameter field (8 CCDs) and a pixel scale of 0.″20/pixel. The short camera mode was used for all our runs. The Lowell's DCT (Happy Jack, Arizona) is equipped with the Large Monolithic Imager (LMI), a 6144 × 6160 pixels CCD (Levine et al. 2012). The field of view is 12.′5 × 12.′5, and 0.″12/pixel is the pixel scale.

We use a range of exposure times between 250 and 900 s, depending on the telescope, the weather conditions, and the filter. Generally, broadband filters[3] are selected to maximize the signal-to-noise ratio of the TNO (VR filter at DCT and WB4800-7800 filter at Magellan). Both filters cover a similar range, near 500–800 nm. Observing details are in Table 1. We applied our usual data calibration, reduction, and analysis (Thirouin et al. 2010; Thirouin & Sheppard 2018). The main steps are as follows: (i) use the bias and dome or twilight flats obtained every night for calibration, (ii) select the optimal aperture radius with the growth curve technique (Howell 1989), (iii) perform the aperture photometry using the DAOPHOT routines with the optimal aperture (Stetson 1987), and (iv) search for periodicity using the Lomb periodogram technique and double-check the result with the Phase Dispersion Minimization (Lomb 1976; Stellingwerf 1978).

3. Photometric Results

In the following section, we present partial/complete light curves for 42 CCs. An example of a partial light curve is shown in Figure 2 and an example of our photometry can be found in Table 3. We divide our sample as follows: (i) light curves showing a large amplitude, (ii) objects with moderate amplitude up to 0.4 mag, (iii) light curves of wide binaries, and (iv) low light-curve amplitudes with a variability lower than 0.2 mag.

3.1. Large-amplitude CCs

Here, we will present three objects with a large light-curve amplitude, suggesting that they are likely contact binaries.

2004 VC_{131}—We observed 2004 VC_{131} over about one month in 2017. We report one isolated night in October obtained with the DCT and three consecutive nights in November with the Magellan-Baade telescope. The main peak of the Lomb periodogram is at 3.06 cycles/day or 7.85 hr (Figure 3). On the basis of the considerations reported in Thirouin et al. (2017), we favor a double-peaked light curve with a 15.7 hr period (Figure 3). The peak-to-peak light-curve amplitude is 0.55 ± 0.04 mag. This large amplitude can be attributed to a contact/close binary or a triaxial ellipsoid. Following the approach described in Thirouin et al. (2017), we derive some physical parameters about 2004 VC_{131} considering a Jacobi ellipsoid and a Roche system.

Assuming a close/contact binary system, we obtain two extreme solutions: (i) a system with a mass ratio of $q_{\rm min} = 0.4$

[3] Transmission curve are at http://www2.lowell.edu/rsch/LMI/specs.html, and http://www.lco.cl/telescopes-information/magellan/operations-homepage/instruments/IMACS/imacs-filters/imacs-filters-1.

Table 1
Orbital Parameters of CCs Observed for This Work and Observing Circumstances: Semimajor Axis (a), Inclination (i), and Eccentricity (e) from the Minor Planet Center (MPC)

TNO	a (au)	e	i (°)	Date UT	#	Δ (au)	r_h (au)	α (°)	Filter	Telescope
(58534) 1997 CQ_{29} Logos–Zoe	45.407	0.118	2.9	2017 Mar 18	3	42.113	43.103	0.1	VR	DCT
2000 CL_{104}	44.447	0.074	1.2	2016 Mar 8	6	42.709	43.700	0.1	VR	Magellan
				2016 Mar 9	7	42.708	43.700	0.1	VR	Magellan
(138537) 2000 OK_{67}	46.581	0.140	4.9	2015 Jul 27	15	39.458	40.121	1.1	VR	DCT
				2015 Aug 20	4	39.211	40.120	0.6	VR	DCT
				2015 Aug 21	9	39.204	40.120	0.6	VR	DCT
				2015 Sep 3	15	39.134	40.119	0.3	VR	DCT
2000 OU_{69}	43.401	0.054	4.4	2015 Aug 19	8	40.115	41.120	0.2	VR	DCT
2001 QS_{322}	43.995	0.039	0.2	2016 Sep 6	19	41.502	42.417	0.6	VR	DCT
(363330) 2002 PQ_{145}	43.982	0.043	3.1	2015 Aug 21	20	44.665	45.674	0.1	VR	DCT
				2015 Sep 3	9	44.707	45.674	0.4	VR	DCT
				2015 Sep 4	6	44.711	45.674	0.4	VR	DCT
(149348) 2002 VS_{130}	44.812	0.120	3.0	2015 Dec 1	8	41.581	42.563	0.1	VR	DCT
				2015 Dec 3	4	41.579	42.563	0.1	VR	DCT
				2015 Dec 4	12	41.576	42.564	0.1	VR	DCT
2003 QE_{112}	43.118	0.040	4.2	2016 Oct 1	7	43.734	44.639	0.6	VR	Magellan
2003 QJ_{91}	44.407	0.038	2.5	2016 Oct 1	7	43.586	44.393	0.8	VR	Magellan
2003 QY_{111}	43.269	0.039	2.9	2017 Oct 28	14	41.533	42.463	0.5	VR	DCT
2003 SN_{317}	42.430	0.045	1.5	2015 Aug 22	4	41.222	41.900	1.0	VR	DCT
2003 YU_{179}	46.546	0.156	4.9	2016 Feb 14	19	39.470	40.424	0.4	VR	DCT
(444018) 2004 EU_{95}	44.443	0.048	2.8	2018 May 17	9	41.546	42.526	0.3	VR	Magellan
				2018 May 18	1	41.550	42.526	0.4	VR	Magellan
2004 HD_{79}	46.295	0.027	1.3	2017 Apr 23	6	46.309	47.175	0.6	r'	Magellan
				2017 Apr 24	12	46.300	47.175	0.6	r'	Magellan
(469610) 2004 HF_{79}	43.623	0.035	1.5	2017 Apr 22	3	41.373	42.221	0.7	r'	Magellan
				2017 Apr 24	11	41.364	42.220	0.7	r'	Magellan
(444025) 2004 HJ_{79}	44.253	0.047	3.3	2018 May 17	4	43.428	44.412	0.3	VR	Magellan
				2018 May 18	9	43.431	44.412	0.3	VR	Magellan
				2018 May 19	3	43.436	44.412	0.3	VR	Magellan
				2019 Feb 2	3	44.405	44.381	1.3	VR	Magellan
				2019 Feb 3	2	44.386	44.380	1.3	VR	Magellan
				2019 Feb 28	5	43.959	44.377	1.2	VR	Magellan
				2019 Mar 1	6	43.944	44.377	1.2	VR	Magellan
				2019 Mar 2	5	43.928	44.377	1.2	VR	Magellan
2004 HP_{79}	48.029	0.191	2.2	2018 May 22	5	37.883	38.877	0.3	VR	DCT
2004 MT_8	43.380	0.036	2.2	2018 May 16	6	44.539	44.926	1.2	VR	Magellan
				2018 May 17	2	44.522	44.926	1.2	VR	Magellan
				2018 May 19	4	44.492	44.926	1.2	VR	Magellan
2004 MU_8	45.131	0.075	3.6	2018 May 18	11	47.259	47.638	1.1	VR	Magellan
				2018 Jun 13	10	46.891	47.635	0.8	VR	DCT
2004 OQ_{15}	43.945	0.129	9.7	2017 Jul 2	13	38.382	39.280	0.7	VR	DCT
2004 PV_{117}	46.348	0.159	4.3	2016 Sep 6	16	39.493	40.455	0.4	VR	DCT
2004 PX_{107}	43.854	0.060	3.0	2017 Jul 3	5	40.991	41.838	0.8	VR	DCT
2004 PY_{107}	44.447	0.101	1.6	2018 Aug 12	4	41.093	42.105	0.1	VR	DCT
2004 VC_{131}	43.728	0.070	0.5	2017 Oct 28	27	39.850	40.759	0.6	VR	DCT
				2017 Nov 21	4	39.772	40.760	0.0	VR	Magellan

Table 1
(Continued)

TNO	a (au)	e	i (°)	Date UT	#	Δ (au)	r_h (au)	α (°)	Filter	Telescope
				2017 Nov 22	3	39.773	40.760	0.0	VR	Magellan
				2017 Nov 23	5	39.773	40.760	0.1	VR	Magellan
2004 VU_{75}	43.543	0.136	3.3	2018 Aug 12	9	43.343	43.624	1.3	VR	DCT
				2018 Oct 6	4	42.741	43.643	0.6	VR	DCT
				2018 Nov 9	8	42.675	43.655	0.2	VR	DCT
				2018 Nov 12	5	42.686	43.656	0.3	VR	DCT
				2018 Nov 13	14	42.690	43.656	0.3	VR	DCT
				2018 Dec 8	4	42.886	43.665	0.8	VR	Magellan
				2018 Dec 9	4	42.897	43.665	0.8	VR	Magellan
				2018 Dec 10	4	42.908	43.666	0.8	VR	Magellan
				2018 Dec 11	4	42.921	43.666	0.9	VR	Magellan
				2018 Dec 12	4	42.933	43.667	0.9	VR	Magellan
2005 EX_{297}	44.053	0.115	4.8	2016 Mar 14	12	43.237	44.198	0.3	VR	DCT
2005 JP_{179}	43.219	0.029	2.1	2018 May 22	2	41.486	42.469	0.3	VR	DCT
				2019 Feb 2	3	42.589	42.485	1.3	VR	Magellan
2005 PL_{21}	46.750	0.153	4.7	2016 Oct 1	7	43.618	44.415	0.8	VR	Magellan
2010 TF_{192}	43.144	0.022	2.3	2017 Oct 28	6	42.480	43.390	0.5	VR	DCT
2010 TL_{182}	43.695	0.056	1.6	2016 Sep 6	17	40.600	41.339	1.0	VR	DCT
2011 BV_{163}	44.013	0.100	4.5	2017 Feb 2	10	38.786	39.771	0.1	VR	DCT
2012 DA_{99}	43.025	0.039	3.2	2018 May 16	5	40.580	41.377	0.9	VR	Magellan
				2018 May 17	1	40.590	41.377	0.9	VR	Magellan
				2019 Feb 2	3	40.956	41.369	1.2	VR	Magellan
				2019 Feb 28	8	40.597	41.369	0.9	VR	Magellan
				2019 Mar 1	8	40.586	41.369	0.9	VR	Magellan
				2019 Mar 2	2	40.576	41.369	0.8	VR	Magellan
2012 DZ_{98}	42.098	0.027	2.8	2018 May 18	6	42.003	42.079	1.0	VR	Magellan
				2018 May 19	3	42.014	42.709	1.0	VR	Magellan
2013 AQ_{183}	46.330	0.159	2.6	2017 Feb 2	8	37.965	38.944	0.2	VR	DCT
				2017 Mar 18	16	38.165	38.944	0.9	VR	DCT
2013 EM_{149}	45.564	0.061	2.6	2018 May 17	9	42.185	43.168	0.3	VR	Magellan
				2018 May 18	1	42.193	42.169	0.3	VR	Magellan
2013 FA_{28}	44.407	0.043	1.5	2017 Feb 2	11	44.669	44.964	1.2	VR	DCT
				2019 Feb 2	4	44.644	44.890	1.2	VR	Magellan
				2019 Feb 3	3	44.629	44.890	1.2	VR	Magellan
				2019 Mar 1	4	44.226	44.888	0.9	VR	Magellan
				2019 Mar 2	5	44.213	44.888	0.9	VR	Magellan
2014 GZ_{53}	44.177	0.042	5.9	2018 May 18	8	41.356	42.321	0.4	VR	Magellan
				2018 May 19	4	41.360	42.321	0.4	VR	Magellan
2014 LQ_{28}	43.662	0.096	1.3	2016 Sep 28	8	38.803	39.790	0.2	VR	Magellan
2014 LR_{28}	44.161	0.052	1.5	2016 Oct 1	7	45.445	46.116	0.9	VR	Magellan
2014 LS_{28}	43.614	0.068	3.8	2017 Apr 22	4	41.230	42.159	0.5	r'	Magellan
				2017 Apr 23	6	41.227	42.159	0.5	r'	Magellan
				2017 Apr 24	8	41.220	42.159	0.5	r'	Magellan
2014 OA_{394}	46.816	0.187	4.4	2016 Sep 28	8	37.438	38.275	0.8	VR	Magellan
2014 OM_{394}	44.001	0.078	2.4	2016 Sep 28	8	45.743	46.741	0.1	VR	Magellan

Note. Our observing circumstances are also reported.

(This table is available in machine-readable form.)

Table 2
We Report Our Findings with the Object's Periodicity (P) and the Full Light-curve Amplitude (Δm)

TNO	P. (hr)	Δm (mag)	ϕ_0 [2450000+ JD]	H (mag)	D (km) 0.04/0.20	Resolved Binary? no/yes/?
(58534) 1997 CQ_{29}	>1.1	>0.5	7830.68212	6.6	318/142	Yes
2000 CL_{104}	>5.5	>0.2	7455.58917	6.2	382/171	No
(138537) 2000 OK_{67}	>6	>0.15	7230.85274	6.2	382/171	No
2000 OU_{69}	>2.5	>0.15	7253.68460	6.6	318/142	No
2001 QS_{322}	>6	>0.3	7637.73440	6.4	349/156	?
(363330) 2002 PQ_{145}	⋯	∼0.1	7255.70248	5.5	528/236	No
(149348) 2002 VS_{130}	⋯	∼0.1	7357.93353	6.3	365/163	?
2003 QE_{112}	⋯	∼0.1	7662.51963	6.6	318/142	?
2003 QJ_{91}	>6	>0.2	7662.50988	6.7	304/136	?
2003 QY_{111}	>5.5	>0.2	8054.64931	6.9	277/124	?
2003 SN_{317}	⋯	∼0.1	7256.94671	6.5	333/149	?
2003 YU_{179}	>5.5	>0.2	7432.60937	6.8	290/130	?
(444018) 2004 EU_{95}	⋯	∼0.1	8255.49186	7.0	265/118	?
2004 HD_{79}	>7	>0.15	7866.84916	5.7	481/215	?
(469610) 2004 HF_{79}	⋯	∼0.15	7865.89661	6.3	365/163	?
(444025) 2004 HJ_{79}	>7.5	>0.20	8255.50327	6.9	277/124	?
2004 HP_{79}	>3	>0.15	8260.72835	6.7	304/136	?
2004 MT_8	>2	>0.2	8254.83578	6.5	333/149	?
2004 MU_8	>2	>0.48	8256.84049	6.0	419/188	Likely contact binary?
2004 OQ_{15}	⋯	∼0.1	7936.84200	6.8	290/130	?
2004 PV_{117}	⋯	∼0.1	7637.63756	6.5	333/149	?
2004 PX_{107}	⋯	∼0.1	7937.87280	7.2	241/108	No
2004 PY_{107}	⋯	∼0.1	8342.76970	6.4	349/156	?
2004 VC_{131}	15.7	0.55 ± 0.04	8054.68366	6.0	419/188	Likely contact binary
2004 VU_{75}[a]	>3	>0.42	8342.83471	6.7	304/136	Likely contact binary?
2005 EX_{297}	⋯	∼0.1	7461.63724	6.1	400/179	?
2005 JP_{179}	⋯	∼0.08	8260.78454	6.4	349/156	?
2005 PL_{21}	>4	>0.15	7662.51333	6.6	318/142	?
2010 TF_{192}	>2.5	>0.3	8054.90005	6.1	400/179	?
2010 TL_{182}	>5.5	>0.25	7637.76776	6.3	365/163	?
2011 BV_{163}	>2.5	>0.15	7786.85122	6.4	349/156	?
2012 DA_{99}	⋯	∼0.1	8254.49418	6.5	333/149	?
2012 DZ_{98}	>5.1	>0.2	8256.48601	6.5	333/149	?
2013 AQ_{183}	>5	>0.15	7786.83242	6.5	333/149	?
2013 EM_{149}	⋯	∼0.1	8255.49759	6.8	290/130	?
2013 FA_{28}	⋯	∼0.1	7786.96917	6.0	419/188	?
2014 GZ_{53}	⋯	∼0.1	8256.53896	6.0	419/188	?
2014 LQ_{28} A	⋯	∼0.08	7659.59329	5.7	481/215	Yes
2014 LQ_{28} B	⋯	∼0.11	⋯	⋯	⋯	⋯
2014 LR_{28}	>4	>0.25	7662.50470	5.0	665/297	?
2014 LS_{28}	11.04	0.35	7865.83999	5.8	460/206	?
2014 OA_{394}	>3	>0.15	7659.58800	6.5	333/149	?
2014 OM_{394}	⋯	∼0.1	7659.60258	5.9	439/196	?

Note. The zero phases without light-time correction (ϕ_0). Absolute magnitudes (H from the MPC) were used to estimate the diameters (D). We also indicate whether the object is a known or not-resolved binary (Stephens & Noll 2006; Noll et al. 2008b). Some objects have not been observed for companion search (to our knowledge); thus, it is unknown whether they are binary, and we used a question mark to identify them

[a] Potential rotational periods of 8.46 hr, 10.2 hr, or 12.9 hr.

(This table is available in machine-readable form.)

and a density of $\rho_{\min} = 1\,\mathrm{g\,cm^3}$ or (ii) a system with a mass ratio of $q_{\max} = 0.5$ and a density of $\rho_{\max} = 5\,\mathrm{g\,cm^3}$. The mass ratio uncertainty is ±0.05. If 2004 VC_{131} has a mass ratio of 0.4, we derive for the primary axis ratios $b_p/a_p = 0.94$ and $c_p/a_p = 0.89$ ($a_p = 130/58$ km, $b_p = 122/55$ km, and $c_p = 116/52$ km with an albedo of 0.04/0.2) and for the secondary axis ratios $b_s/a_s = 0.86$ and $c_s/a_s = 0.81$ ($a_s = 102/46$ km, $b_s = 88/40$ km, and $c_s = 83/37$ km, albedo of 0.04/0.2). With $D = 0.6$, the separation between the components is 387/174 km for an albedo of 0.04/0.2. This study is summarized in Figure 3. As a density of $5\,\mathrm{g\,cm^3}$ is not likely in the Kuiper Belt, we do not consider this option here, but basic parameters derived assuming such a density are available in Figure 3 (Thirouin & Sheppard 2017).

In the case of a Jacobi ellipsoid and considering an equatorial view, the object's elongation is $a/b = 1.66$ and $c/a = 0.44$ (Chandrasekhar 1987). We find $a = 353$ km ($a = 158$ km), $b = 213$ km ($b = 95$ km), and $c = 155$ km ($c = 70$ km)

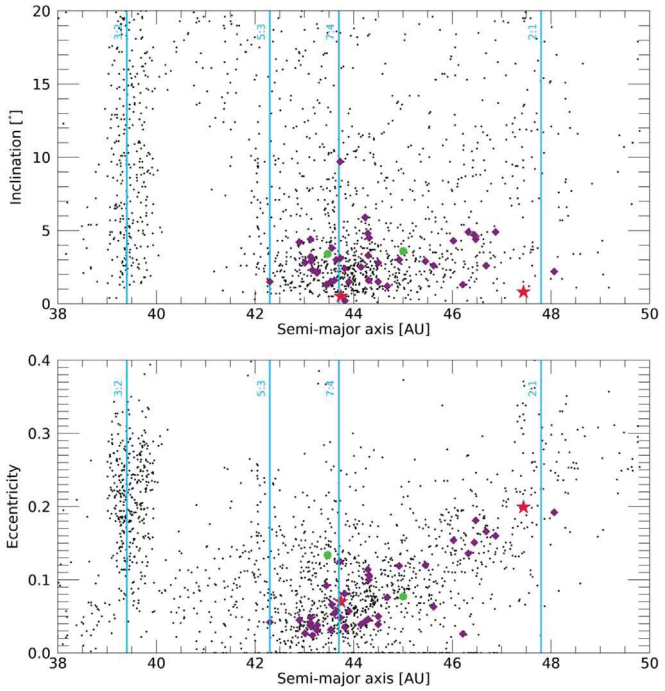

Figure 1. Black dots are all the TNOs discovered with semimajor axes from 38 to 50 au. Purple diamonds are the CCs with partial/complete light curves reported in this work, red stars are the two likely contact binaries with full light curves, 2002 CC_{249} (Thirouin & Sheppard 2017) and 2004 VC_{131} (this work), and green circles indicate two candidates for likely contact binaries, 2004 MU_8 and 2004 VU_{75} (this work). Blue continuous lines are the 3:2, 5:3, 7:4, and 2:1 Neptune's resonances. Orbital elements available at the Minor Planet Center (MPC, 2018 November).

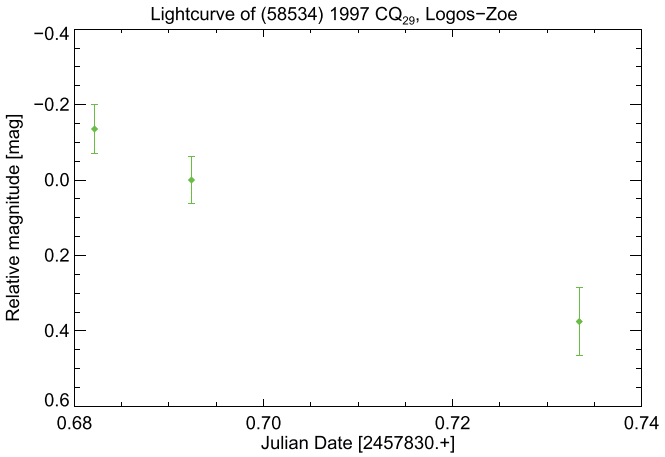

Figure 2. Example of a partial light curve.

(The complete figure set (39 images) is available.)

for an albedo of 0.04 (0.20). The viewing angle of 2004 VC_{131} has to be larger than 62°.5 to avoid an axis ratio $a/b > 2.31$ (Jeans 1919). Considering an equatorial view, the density is $\rho \geqslant 0.17\ \mathrm{g\ cm^3}$ (Chandrasekhar 1987).

2004 VU_{75}—We observed 2004 VU_{75} on several occasions with the DCT. Our first partial light curve was obtained in 2018 August over approximately 3 hr for a variability of 0.42 mag. Our August data correspond to the minimum of the curve, which seems to be a sharp minimum with a V shape. We reobserved this object in November over three nonconsecutive nights. Unfortunately because of bad weather, we can only report fragmentary data sets (Figure 4). In 2018 December, we reobserved 2004 VU_{75} over five consecutive nights with the Magellan-Baade telescope. We performed a search for rotational period using all our data or only the high-quality data and found three potential double-peaked periodicities of 12.9, 10.2, and 8.4 hr. We favor the double-peaked periodicity on the basis of the large amplitude. With a range of 8–13 hr, this object seems to have a moderate rotational period. Based on the large variability and the sharp minimum of our first light curve, we have some hints that 2004 VU_{75} is perhaps a contact binary. Therefore, more observations to confirm the nature of this object are highly desirable.

Table 3
Photometry Used in This Paper Is Available in the Following Table

Object	Julian Date	Relative Magnitude (mag)	Error (mag)
(58534) 1997 CQ_{29} Logos–Zoe			
	2457830.68213	−0.14	0.07
	2457830.69215	0.00	0.06
	2457830.73353	0.38	0.09
2000 CL_{104}			
	2457455.58917	0.074	0.10
	2457455.59440	0.052	0.11
	2457455.74390	−0.07	0.12
	2457455.81342	−0.05	0.09
	2457456.61859	−0.01	0.09
	2457456.62435	0.08	0.09
	2457456.64539	0.05	0.09
	2457456.65107	−0.04	0.10
	2457456.71587	−0.11	0.09
	2457456.75722	0.01	0.10

Note. Julian date is without light-time correction.

(This table is available in its entirety in machine-readable form.)

2004 MU_8—We observed 2004 MU_8 on two occasions with the Magellan Telescope in 2018 May and with the DCT in 2018 June Figure 5. Over about 2.5 hr at DCT and ∼2 hr at Magellan, 2004 MU_8 displayed a variability of 0.33 mag and 0.48 mag, respectively. Unfortunately, we do not have enough data to cover the full rotation of this object and so derive its periodicity. We can only infer that the period is larger than 2.5 hr and that the amplitude is larger than 0.48 mag. On the basis of the large amplitude over a short amount of time, 2004 MU_8 is a good candidate to the likely contact binary category. There is no information in the literature about a search for satellites orbiting 2004 MU_8.

3.2. Moderate-amplitude CCs

This subsection is dedicated to the CCs displaying a moderate light-curve amplitude. Objects with a variability above 0.3 mag are potentially interesting targets for follow-up observations at different epochs to look for changes.

2014 LS_{28}—From three consecutive nights of observations with the Magellan-Baade telescope in 2017 April, we estimate that the periodicity of 2014 LS_{28} is 11.04 hr and the amplitude is 0.35 ± 0.03 mag. The single-/double-peaked light curves with rotational periods of 5.52 hr/11.04 hr, respectively, are plotted in Figure 6. The Lomb periodogram presents several

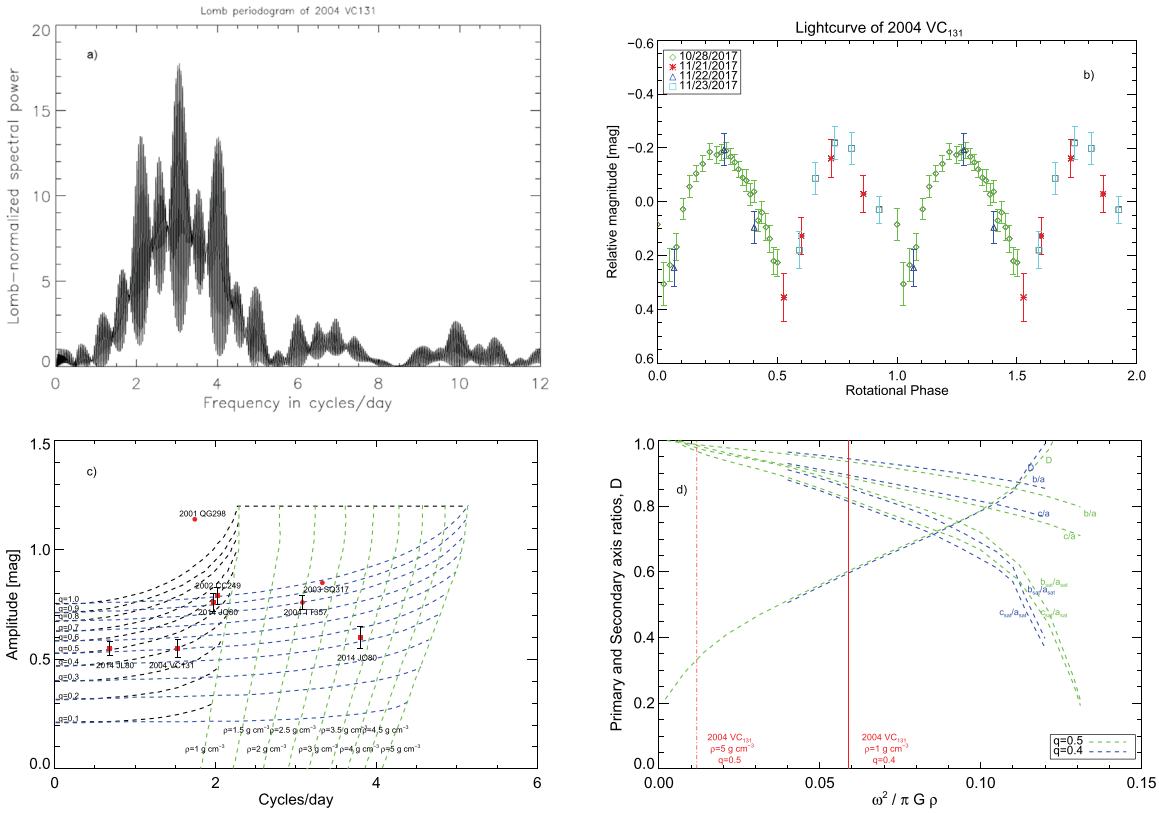

Figure 3. Study of 2004 VC_{131}. The Lomb periodogram (plot a)) has one main peak, suggesting a rotational period of 2×7.85 hr (plot b)). The rotational phase of the light curve is between 0 and 2, and so two rotations are plotted. With plots (c) and (d), we calculated the potential mass ratios, size, and shape of the components, density, and separation (D) for a contact binary configuration.

aliases of the main peak (Figure 6). To our knowledge, there was no satellite search for 2014 LS_{28}.

Assuming that 2014 LS_{28} is a triaxial object with $a > b > c$ and an equatorial view, we derive $b/a = 0.72$ and $c/a = 0.49$. The density is $\rho \geqslant 0.33$ g cm^{-3}. Detailed procedures regarding the estimate of these values are available in Thirouin et al. (2010, 2012).

(444025) 2004 HJ_{79}—On the basis of three consecutive nights, 2004 HJ_{79} shows a possible steep slope suggesting an amplitude larger than 0.20 mag. However, the rest of the curve is mostly flat. We reobserved this object in 2019 February and March. The light curve displays similar behavior. As the amplitude is about 0.20 mag over consecutive nights, we use this value in this study. We infer that the periodicity is larger than 7.5 hr. No resolved binary search is available for this object.

2010 TF_{192}—Over ∼2.5 hr of observations, 2010 TF_{192} has a variability of about 0.3 mag. Our partial light curve displays a minimum and a maximum, suggesting that the amplitude of the full light curve is likely not much greater than 0.3 mag. There is no information in the literature about a satellite search for this object.

2010 TL_{182}–In about 5.5 hr, 2010 TL_{182} displays a variability of about 0.25 mag. To our knowledge, no search for companion was performed for this object.

2014 LR_{28}—In a little less than 4 hr, 2014 LR_{28} has a variability of about 0.25 mag. 2014 LR_{28} is the largest object in our sample and one of the largest objects in the CC population. As we will discussed in the Section 4, all the large TNOs are resolved wide binaries (Noll et al. 2014). However, no search for satellite has been done for this object. Therefore, it would be interesting to confirm the presence of a companion and infer whether the amplitude is due to an asynchronous state.

3.3. Wide Binary CCs

Resolved wide binaries are not the main topic of our survey, but we observed Logos–Zoe to confirm a potential large variability and discovered a new wide binary, 2014 LQ_{28}.

(58534) 1997 CQ_{29}, Logos–Zoe—Logos was discovered in 1997 from Maunea Kea, and its satellite, Zoe, was identified in *HST* images by Noll et al. (2002). Zoe's orbit is well characterized with an orbital period of 309.9 days, a semimajor axis of 8220 km, an eccentricity of 0.55, and an inclination of 95°.4 (Grundy et al. 2011; Noll et al. 2004). Logos has an estimated diameter of 80 km, and Zoe is a 66 km diameter object (Noll et al. 2004). Noll et al. (2008a) reported a high variability for Logos on the basis of *HST* data; however, because of the sparse sampling, there is no constraint for the rotational period. In 2017 March, we observed Logos–Zoe for about 1 hr and confirm a large variability with $\Delta m > 0.5$ mag.

2014 LQ_{28}—We observed 2014 LQ_{28} during 5.5 hr with the Magellan-Baade telescope in 2016 September. During our observing run, the seeing was 0.″4 allowing the discovery of a companion orbiting this object. The magnitude difference between the two components is about 0.4 mag, and their separation was 0.″86 (Sheppard & Thirouin 2018). The system was reobserved in 2017 October to confirm the binarity, and this time the separation was 0.″36. The components variability are about the same of ∼0.1 mag over 5.5 hr.

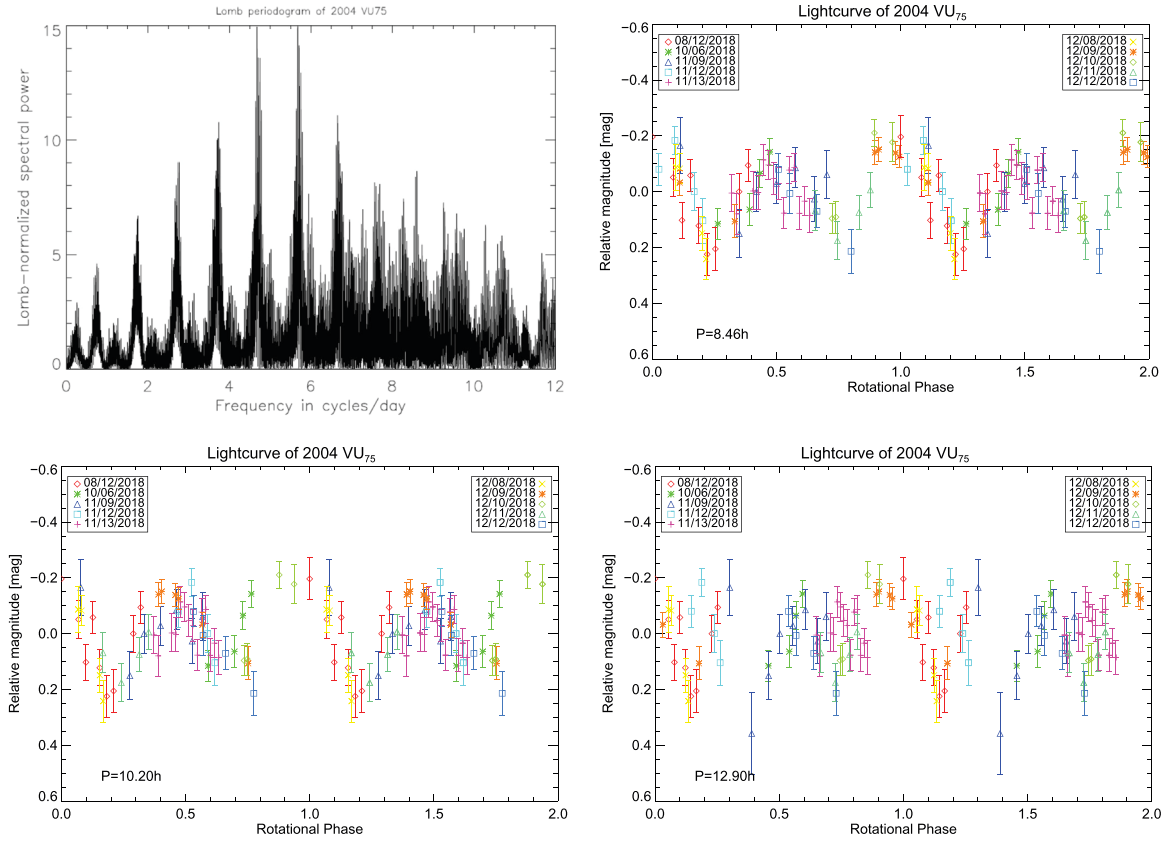

Figure 4. Lomb periodogram using all our data favors a single-peaked light-curve rotational period of 4.23 hr or 5.13 hr for 2004 VU_{75}, which would be a double-peaked rotational period of 8.46 hr or 10.2 hr. Using only our Magellan data, Lomb periodogram favors a single-peaked light curve with $P = 6.45$ hr (double-peaked of 12.9 hr). The best fit is obtained assuming a rotation of 8.46 hr (upper right plot).

3.4. Low-amplitude CCs

Finally, we report objects with a low light-curve amplitude. If an object shows signs of variability ($\Delta m > 0.15$ mag), we will use the duration of our observing as lower limit for the rotational period and the variability as lower limit of the light-curve amplitude. If the light curves are too noisy and/or flat ($\Delta m < 0.15$ mag), we will report an approximate amplitude. Such low-amplitude light curves can be attributed to a nearly spherical object with limited albedo variations on its surface, a pole-on oriented object, or a very slow rotator with a variability (and periodicity) undetectable over the duration of our observing block (Sheppard et al. 2008; Thirouin et al. 2014). Therefore, the duration of our observing block cannot constrain the object's periodicity, as we do not know the reason of the flat light curve. Only if the object is a slow rotator, then can our observing block duration be a lower limit.

2000 CL_{104}—In 2016 March, we observed 2000 CL_{104} during two consecutive nights with the Magellan-Baade telescope. The duration of the observing blocks are about 5.5 and ∼3.2 hr, respectively. Both nights show a similar variability of about 0.2 mag. We can infer that the rotation is probably longer than 5.5 hr. To our knowledge, there is no other published light curve for 2000 CL_{104}. No companion was found orbiting this object (Noll et al. 2008b).

(138537) 2000 OK_{67}—Between 2015 July and September, four nights were dedicated to the observations of 2000 OK_{67} with the DCT. This object has a low variability of about 0.15 mag, consistent over all observing nights. Our longest observing block is ∼6 hr. Noll et al. (2008b) reported no companion for 2000 OK_{67}.

2000 OU_{69}—In 2015 August, we observed 2000 OU_{69} for about 2.5 hr. The light curve presents a low variability of about 0.15 mag. To our knowledge, we report here the first light curve for this object. According to Noll et al. (2008b), 2000 OU_{69} has no satellite.

2001 QS_{322}—With an observing block of about 6 hr, we report a partial light curve with a variability of about 0.15 mag for 2001 QS_{322}. No companion search was performed for this object.

(363330) 2002 PQ_{145}—We dedicated three observing nights to 2002 PQ_{145} between 2015 August and September. We report a very low variability light curve with Δm ∼0.1 mag. Our longest observing run is about 5.5 hr. Noll et al. (2008b) found no evidence for a companion orbiting 2002 PQ_{145}.

(149348) 2002 VS_{130}—With three observing nights in 2015 December with the DCT, we are not able to derive the periodicity. On the basis of our longest observing run of 3.5 hr, the light-curve amplitude is ∼0.1 mag. To our knowledge, no companion search was performed for 2002 VS_{130}.

2003 QE_{112}—With one night of data from the Magellan-Baade telescope, we report a low variability of about 0.1 mag over the duration of our observing block, which is ∼5 hr. To our knowledge, no observation to search for satellite has been performed for this object.

2003 QJ_{91}—We present seven images of 2003 QJ_{91} obtained over approximately 6 hr. This object shows a variability of about 0.2 mag. We report here the first variability

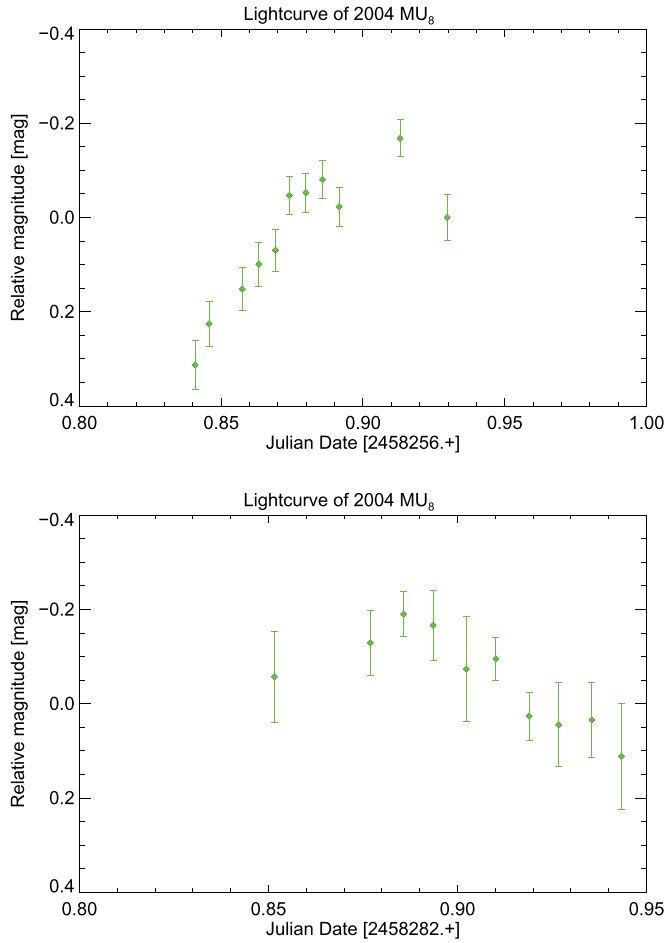

Figure 5. Partial light curves obtained with the Magellan-Baade telescope (upper plot) and with the DCT (lower plot). In both cases, 2004 MU_8 displays a large amplitude in a few hours thus, it is a good candidate for likely contact binary. More data are required to obtain the full light curve and infer the nature of the object/system.

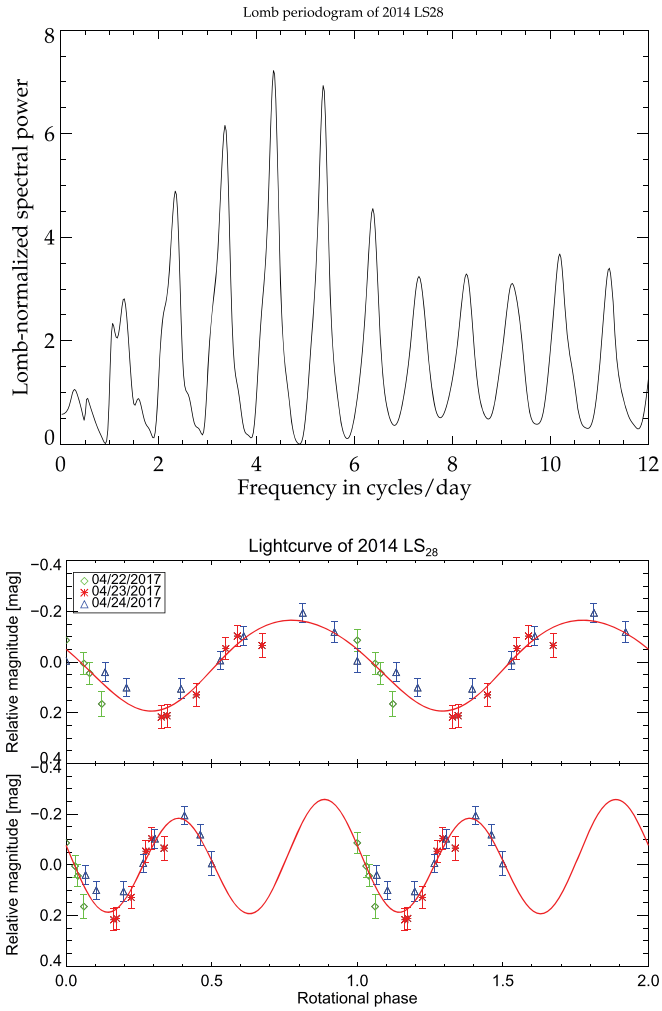

Figure 6. Lomb periodogram for 2014 LS_{28} has one main peak at 4.37 cycles/day and several aliases. The lower plots are the single- and double-peaked light curves assuming the main peak as rotational period.

measurements for 2003 QJ_{91}. No search for satellite has been published.

2003 QY_{111}—Santos-Sanz et al. (2009) observed 2003 QY_{111} with the Very Large Telescope in November 2003 for a *BVRI* color study. They report a potential short-term variability of 0.72 mag over 156 minutes (see Table 4 in Santos-Sanz et al. 2009). To confirm such a large variability, we reobserved this object with the DCT in 2017 October. After 5.5 hr of observations, we report a variability of about 0.2 mag. Therefore, the large amplitude noticed by Santos-Sanz et al. (2009) is unconfirmed. Assuming that this amplitude noticed in 2003 is correct, one can argue that the spin axis orientation of 2003 QY_{111} changed significantly to see a different light-curve amplitude in 2017. Similarly, if 2003 QY_{111} is a close binary, the system's configuration would have changed significantly in about 14 yr (Lacerda 2011). However, Santos-Sanz et al. (2009) focused on colors, and, thus, their images were not the best suited for light-curve analysis. To our knowledge, 2003 QY_{111} was not observed for a resolved companion.

2003 SN_{317}—2003 SN_{317} was observed for less than 1 hr with the DCT in 2015 August. The partial light curve has an amplitude of about 0.1 mag. No search for a satellite or other light curve has been reported in the literature for this object.

2003 YU_{179}—On the basis of 5.5 hr of data obtained in 2016 February, we cannot derive a secure rotational period for 2003 YU_{179}. The partial light curve displays an amplitude of about 0.2 mag. There is no report in the literature about a search for resolved companion orbiting this object.

2004 EU_{95}—Images of 2004 EU_{95} were obtained over two consecutive nights with the Magellan telescope. With 8 hr of data, the amplitude is about 0.1 mag. No literature is available about a search for resolved binary.

2004 HD_{79}—We report two consecutive nights with the Magellan-Baade telescope in 2017 April. Our longest observing block is about 7 hr. As there is no clear repetition in the photometry, the period is likely larger than 8 hr. The amplitude is about 0.15 mag. To our knowledge, 2004 HD_{79} has not been inspected for a resolved companion.

(469610) 2004 HF_{79}—On the basis of two consecutive observing nights, we cannot derive a secure period for this object. We constrain the periodicity to be larger than 7.5 hr, and the amplitude is about 0.15 mag. To our knowledge, 2004 HF_{79} has not been observed for a companion search.

2004 HP_{79}—We obtained five usable images of 2004 HP_{79} with the DCT, suggesting a light-curve variability of

~0.15 mag and a periodicity longer than 3 hr. This object has not been observed for companion detection.

2004 MT_8—We observed this object over three consecutive nights during approximately 2 hr every night. Each block is showing a low variability, but it seems that 2004 MT_8 has a variability of about 0.2 mag over the three nights. On the basis of our short observing blocks, we cannot exclude a short-term variability and, thus, we can only constrain the periodicity to be longer than 2 hr. No satellite search was performed for this object on the basis of the literature available.

2004 OQ_{15}—We observed 2004 OQ_{15} for about 2.5 hr with the DCT. This object displays a variability of about 0.1 mag. No search for a companion has been performed for this object.

2004 PV_{117}—The variability of 2004 PV_{117} is low, about 0.1 mag over 3 hr. No information about a satellite search is reported in the literature.

2004 PX_{107}—Noll et al. (2008b) searched for a companion orbiting 2004 PX_{107}. They report no satellite according to their data. We observed this object in 2017 July with the DCT. Our observing block is about 1.5 hr. There is no clear variability according to our data (amplitude ~0.1 mag).

2004 PY_{107}—In 2018 August, we observed 2004 PY_{107} during approximately 2 hr, and we report a low-amplitude light curve of 0.1 mag. This object was not inspected for binarity.

2005 EX_{297}—We observed 2005 EX_{297} during one night in 2016 March. On the basis of our data obtained over ~6 hr, the light-curve variability is only about 0.1 mag. There is no published information about a satellite search for this object.

2005 JP_{179}—With only two images of 2005 JP_{179} obtained in 2018, we report that the variability is larger than 0.08 mag. This amplitude is consistent with our 2019 data. There is no indication in the literature for a binary search.

2005 PL_{21}—In about 4 hr of data obtained with the Magellan-Baade telescope in 2016, we cannot secure a rotational period for 2005 PL_{21}. The partial light curve reported here presents a low amplitude of about 0.15 mag. This object has not been the topic of a search for companion.

2011 BV_{163}—We report ~2.5 hr of data for 2011 BV_{163} obtained with the DCT in 2017 February. The partial light curve has a variability of about 0.15 mag. We present here the first light curve for this object. No search for satellite has been done for 2011 BV_{163}.

2012 DA_{99}—In 2018 May, we obtained images of 2012 DA_{99} with the Magellan-Baade telescope over two nights. This object shows a low variability (~0.1 mag) in about 2.2 hr. Data obtained in 2019 February and March at Magellan over minutes, hours, and days confirm the low variability. 2012 DA_{99} has not been imaged for a resolved companion.

2012 DZ_{98}—Over about 5 hr, 2012 DZ_{98} displays a variability of ~0.2 mag. There is no indication in the literature about a resolved binary search.

2013 AQ_{183}—From two nights of observations in 2017 February and March, we cannot derive a secure rotational period for 2013 AQ_{183}. Our longest observational run is about 5 hr, and, thus, we infer that the periodicity is longer than 5 hr. Both nights present the same variability, about 0.15 mag. No satellite search has been done for 2013 AQ_{183}.

2013 EM_{149}—In more than 7 hr of observations, 2013 EM_{149} has a very low variability of only 0.1 mag. No companion search has been performed for this object.

2013 FA_{28}—On the basis of our ~2 hr of observations for 2013 FA_{28} obtained in 2017 February, we report a low variability of about 0.1 mag. Similar variability is noticed over minutes, hours, and days in both of our data sets obtained in 2019 February–March. To our knowledge, no search for satellite orbiting 2013 FA_{28} was performed.

2014 GZ_{53}—In ~8 hr, 2014 GZ_{53} shows a very low variability of about 0.1 mag. This object has not been imaged for satellite search.

2014 OA_{394}—With only four usable images of 2014 OA_{394} obtained over about 3 hr, we are not able to estimate a periodicity. The partial light curve displays an amplitude of about 0.15 mag. There is no information available regarding a search for companion.

2014 OM_{394}—We observed 2014 OM_{394} with the Magellan-Baade telescope over approximately 5.5 hr in 2016 September. The partial light curve reported here presents a very low variability, about 0.1 mag. There is no derived rotational period according to our data. To our knowledge, this object has never been the topic of a search for satellite.

4. Rotational Characteristics of the CCs

4.1. Light Curves: Our Sample and Published Results

Table 4 summarizes all the published light curves of the CC population. About 900 CCs are known, but only 43 have been observed for rotational variability (without taking into account our survey), and 10 of them (24% of the sample) are in fact known wide binaries. The light curve of a binary system can be resolved or unresolved. In other words, the two systems' components can be separated, and, thus, there is one light curve for each component or the components are unresolved and the reported photometry in the photometry of the pair. Resolved ground-based light curves are challenging and require excellent weather conditions to separate the components, as well as systems with large separation and large-aperture facilities. For those reasons, most of the binary system light curves are unresolved (Thirouin et al. 2014). Only two attempts of resolved light curves with the 6.5 m Magellan Telescope have been published for Teharonhiawako-Sawiskera ((88611) 2001 QT_{297}) and 2003 QY_{90} (Osip et al. 2003; Kern & Elliot 2006).

Over the past years, the main effort to study the rotational properties of the CCs has been focused on the binaries. However, binaries undergo tidal effects affecting the rotations of the components; thus, their rotational properties are not primordial and, therefore, not representative of the CC population (Thirouin et al. 2014). Several objects that we and other teams imaged have not been observed for companion search, and, thus, we do not know whether they are wide binaries (e.g., 2002 GV_{31},[4] 2003 QY_{111}).

The main focus on light curves of wide binary CCs created a bias in our understanding of the rotational properties of the CC population. Therefore, for the purpose of this work, we focus on the single CCs. It is important to mention that some of the reported CCs have not been observed for satellites with *HST*, so some of them could be wide binary systems (see Table 2 for a complete review). Only the known binary Logos–Zoe was selected because we wanted to confirm the large amplitude

[4] With a long rotational period of about 29 hr and a relatively large size of $H = 6.4$ mag, 2002 GV_{31} is potentially a binary system (Thirouin et al. 2014; Pál et al. 2015)

Table 4
Summary of the Published Light-curve Studies of the Dynamically CC TNOs

TNO	*P*. (single) (hr)	*P*. (double) (hr)	Δm (mag)	*H* (mag)	References
(19255) 1994 VK_8[a]	3.9/4.3/4.7/5.2	7.8/8.6/9.4/10.4	0.42	7.0	RT99
	4.75	⋯	⋯	⋯	CB99
(58534) 1997 CQ_{29} Logos–Zoe[b]	⋯	⋯	∼0.8	6.6	N08
(79360) 1997 CS_{29} Sila–Nunam[b]	⋯	⋯	<0.08	5.3	SJ02
	⋯	⋯	<0.22	⋯	RT99
	150.1488	300.2388	0.120 ± 0.012/0.044 ± 0.010	⋯	R14
	⋯	⋯	0.14 ± 0.07	⋯	G12, BS13
(66652) 1999 RZ_{253} Borasisi-Pabu[b]	⋯	⋯	<0.05	5.9	LL06
	6.4 ± 1.0	⋯	0.08 ± 0.02	⋯	K06
(80806) 2000 CM_{105}[b]	⋯	>3	<0.14	6.6	LL06
(88611) 2001 QT_{297} Teharonhiawako[b]	⋯	⋯	<0.15	5.8	O03
	5.50 ± 0.01 or 7.10 ± 0.02	11.0 ± 0.02 or 14.20 ± 0.04	(0.32 or 0.30) ± 0.04	⋯	K06
(88611B) 2001 QT_{297} B Sawiskera[b]	4.75	⋯	0.6	⋯	O03
	4.749 ± 0.001	9.498 ± 0.02	0.48 ± 0.05	⋯	K06
(275809) 2001 QY_{297}[b]	5.84	11.68	0.49 ± 0.03	5.4	T12
	12.2 ± 4.3	⋯	0.66 ± 0.38	⋯	K06
(126719) 2002 CC_{249}[c]	⋯	11.87 ± 0.01	0.79 ± 0.04	6.6	TS17
2002 GV_{31}	⋯	29.2	0.35 ± 0.06	6.4	P15
2002 VT_{130}[b]	⋯	>4	>0.21	5.6	T14
2003 BF_{91}[d]	**9.1**/7.3	⋯	1.09 ± 0.25	11.7	TB06
2003 BG_{91}[d]	**4.2**/4.5/4.6/4.9	⋯	0.18 ± 0.075	10.7	TB06
2003 BH_{91}[d]	2.8	⋯	<0.15	11.9	TB06
2003 FM_{127}	6.22 ± 0.02	⋯	0.46 ± 0.04	7.1	K06
2003 $QY_{90}A$[b]	3.4 ± 1.1	⋯	0.34 ± 0.12	6.4	KE06
2003 $QY_{90}B$[b]	7.1 ± 2.9	⋯	0.90 ± 0.36	⋯	KE06
2003 QY_{111}	⋯	>2.5	0.72	6.9	SS09
2005 EF_{298}[b]	**4.82**/6.06	**9.65**/12.13	0.31 ± 0.04	5.9	BS13
(303712) 2005 PR_{21}[b]	⋯	>5.5	<0.28	6.2	BS13
2013 SM_{100}	⋯	>5	>0.60	8.5	A18
2013 UC_{18}	⋯	>5	>0.44	8.3	A18
(505476) 2013 UL_{15}	⋯	>5	>0.36	6.6	A18
2013 UP_{15}	⋯	>5	>0.29	7.5	A18
2013 UR_{22}	⋯	>5	>0.44	7.8	A18
2013 UY_{16}	⋯	>5	>0.36	7.6	A18
2013 UN_{15}	⋯	>5	>0.56	7.3	A18
2013 UW_{16}	⋯	>5	>0.11	7.3	A18
2013 UW_{17}	⋯	>5	>0.40	7.6	A18
2015 RA_{280}	⋯	>6	>0.61	7.6	A18
2015 RB_{280}	⋯	>6	>0.55	7.6	A18
2015 RB_{281}	⋯	>5	>0.42	7.4	A18
2015 RC_{280}	⋯	>6.5	>0.40	9.0	A18
2015 RE_{280}	⋯	>6	>0.20	7.9	A18
2015 RH_{280}	⋯	>6	>0.38	9.0	A18
2015 RH_{281}	⋯	>6	>0.44	8.4	A18
2015 RK_{281}	⋯	>6	>0.21	8.6	A18
2015 RO_{281}	⋯	>6	>0.35	7.5	A18
2015 RP_{281}	⋯	>6	>0.42	7.7	A18
2015 RQ_{280}	⋯	>6	>0.30	8.8	A18
2015 RT_{279}	⋯	>6	>0.40	8.2	A18
2015 RW_{279}	⋯	>6.5	>0.20	8.2	A18
2015 RZ_{279}	⋯	>5	>0.27	7.6	A18
uo3l88[e]	⋯	>5	>0.50	8.3	A18
uo5t55[e]	⋯	>6	>0.30	8.7	A18

Notes. In case of multiple values, the preferred one, according to the authors of each study, is indicated in bold.

[a] Thanks to *HST* observations, no companions have been detected for 1994 VK_8 (Noll et al. 2008b).

[b] Known resolved binary systems. In some cases, the primary and the satellite have been observed separately and a light curve for each is available; thus, we indicate both values individually.

[c] Likely a contact binary (Thirouin & Sheppard 2017).

[d] The light curves of 2003 BG_{91}, 2003 BF_{91}, and 2003 BH_{91} were obtained with *HST* (Trilling & Bernstein 2006). The light curve of 2003 BH_{91} presents a very high dispersion, and a rotational period of 2.8 hr seems unlikely (Sheppard et al. 2008; Thirouin 2013), and Trilling & Bernstein (2006) were not confident about this result. Therefore, 2003 BH_{91} is not considered for the purpose of this work.

[e] uo3l88 and uo5t55 are not fully characterized by the OSSOS survey yet and, thus, have not been submitted to the MPC and have no official designation.

References list. CB99: Collander-Brown et al. (1999); RT99: Romanishin & Tegler (1999); SJ02: Sheppard & Jewitt (2002); O03: Osip et al. (2003); KE06: Kern & Elliot (2006); K06: Kern (2006); LL06: Lacerda & Luu (2006); TB06: Trilling & Bernstein (2006); N08: Noll et al. (2008b); SS09: Santos-Sanz et al. (2009); G12: Grundy et al. (2012); T12: Thirouin et al. (2012); BS13: Benecchi & Sheppard (2013); R14: Rabinowitz et al. (2014); T14: Thirouin et al. (2014); P15: Pál et al. (2015); TS17: Thirouin & Sheppard (2017); A18: Alexandersen et al. (2018).

reported in Noll et al. (2008a). In the case of 2014 LQ_{28}, we discovered during the Magellan observations that this object is an equal-sized wide binary (see Section 3).

Noll et al. (2014) reported that 100% of the bright CCs ($H \lesssim 6$ mag) are binary systems. Mainly, we select CCs with an absolute magnitude $H > 6$ mag, but as we do not want to bias our sample toward "small" size objects, we also select a couple of larger CCs. Therefore, several large CCs in our sample are perhaps wide binaries. We estimate that up to five CCs with $H < 6$ mag (2004HD_{79}, 2004 HF_{79}, 2014 LR_{28}, 2014 LS_{28}, and 2014 OM_{394}) could be wide binaries according to the criteria of Noll et al. (2014). The cutoff at $H < 6$ mag is approximate, and so objects with an absolute magnitude around the cutoff could be wide binaries (e.g., 2013 FA_{28}). Because of their recent discoveries, the Alexandersen et al. (2018) targets have never been search for resolved binaries, but according to their small sizes, we do not expect them to be resolved binary systems (Noll et al. 2008a, 2014; Penteado et al. 2016). Ultimately, only a search for resolved companion with the *HST* and/or the *James Webb Space Telescope* will confirm the nature of theses objects/systems.

Also, the brightest and, thus, the largest CCs (typically, $H < 6$ mag) have been studied for light curves as they are the easiest ones to observe. Therefore, our survey is focused on smaller objects with an absolute magnitude up to 7.2 mag. Recently, Alexandersen et al. (2018) observed objects up to 9.2 mag taking advantage of the large aperture of the Subaru telescope. Alexandersen et al. (2018) observed TNOs discovered by the Outer Solar System Origins Survey (OSSOS) in all dynamical groups, and only 25 objects in their sample belong to the CC population (see Table 2 of Alexandersen et al. 2018). The maximum amplitude variation reported by Alexandersen et al. (2018) is the difference between the brightest and the faintest data point. In some cases, the light curves present a high dispersion and some points are outliers. Therefore, we reestimated such amplitudes with conservative values by taking into account potential outliers and removing them for the estimates (Table 4).

The smallest CCs observed for light-curve variability with the *HST* are 2003 BF_{91} with $H = 11.7$ mag, 2003 BG_{91} with $H = 10.7$ mag, and 2003 BH_{91} with $H = 11.9$ mag (Trilling & Bernstein 2006). These objects are in the same size range as 2014 MU_{69} with $H = 11.1$ mag. In the case of 2003 BH_{91}, no reasonable rotational period was derived, and so this object will not be considered in our work. For 2003 BF_{91}, a single-peaked light curve with $P = 9.1$ hr and a $\Delta m = 1.09$ mag was preferred, but 7.3 hr was also a possibility. By assuming a single-peaked light curve, it is considered that 2003 BF_{91} is a spheroidal object with albedo variation of its surface. However, a variability of 1.09 mag suggests very strong albedo variegation (s) on the objects surface, which is doubtful. Therefore, a more appropriate option is to consider an ellipsoidal object with a double-peaked light curve. On the basis of the photometry and the two potential rotational periods reported by Trilling & Bernstein (2006), the best light curve is found using a periodicity of 2×7.3 hr (value used for the rest of our study) with 1.01 mag as amplitude. On the basis of the large variability, 2003 BF_{91} is a likely contact binary, but one has to keep in mind that the light curve is very noisy (Trilling & Bernstein 2006). For 2003 BG_{91}, Trilling & Bernstein (2006) selected a single-peaked period of 4.2 hr. On the basis of the supposed fast rotation, it is likely that 2003 BG_{91} is highly elongated; however, the amplitude reported is only 0.18 mag. Therefore, it is more likely that the double-peaked light curve with a period of 2×4.2 hr is more appropriate (solution used in this work).

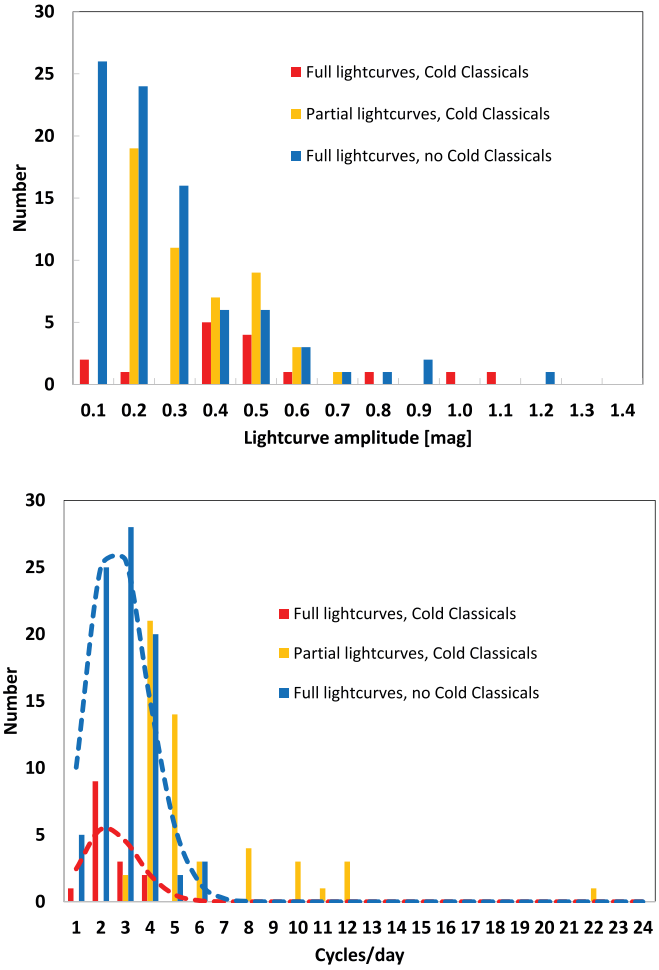

Figure 7. Histograms using the partial and full light curves reported in this work and the literature. The CCs tend to have more amplitude than the rest of the TNOs. The blue discontinuous line is a Maxwellian fit using only the CC full light curves, suggesting a mean rotational period of 2.53 cycles/day (9.48 hr), whereas the red discontinuous line is for the other TNOs with a mean period of 8.45 hr.

In conclusion, the published literature and our survey are focused on a wide range of sizes (5.0 mag $\geqslant H \geqslant$ 11.9 mag), and, thus, by merging these results, we can infer the rotational properties of the entire CC population, as well as probe the properties of different size regimes (Table 4).

4.2. Light-curve Amplitude and Rotational Period Distributions

In Figure 7, we summarize the light-curve studies of the CC population by taking into account the full and partial light curves. For the partial light curves, we only have access to the lower limits for the rotational period and the light-curve amplitude, whereas the full light curve provides us with an exact estimate for both parameters. Flat light curves from this work are not plotted.

On the basis of the 16 full light curves available in the literature and this work, we report that the mean light-curve amplitude is about 0.39 mag, whereas the partial light curves have a mean amplitude of 0.29 mag (0.20 mag with the flat

light curves). On the basis of TNO light curves from all dynamical groups, Duffard et al. (2009) reported that 70% of them have a low variability, $\leqslant$0.2 mag. On the basis of an updated and larger sample, we estimate that ~65% of the other TNOs have an amplitude <0.2 mag. Only 36% of the CCs have an amplitude lower than 0.2 mag (including the flat light curves). Therefore, the CCs tend to have more amplitude, suggesting that they are more elongated or present a higher deformation than the rest of the TNOs. As the sample of full light curves is dominated by resolved binaries, the larger amplitude can be attributed to the formation of these systems (Thirouin et al. 2014). However, on the basis of our sample of partial light curves likely dominated by single objects and unresolved binaries, such a tendency remains. Therefore, the larger amplitude can potentially be a primordial characteristic of the CC population.

The period distributions with the full and partial light curves from our survey and the literature are also plotted in Figure 7 (flat light curves are not included). Considering only the full light curves, the Maxwellian distribution fit infers a mean period of 9.48 $\pm$ 1.53 hr. Duffard et al. (2009), Thirouin et al. (2010), and Benecchi & Sheppard (2013) calculated a mean rotational period of the entire TNO population of 7–8 hr. Using an updated sample, the mean rotational period of the other TNOs is 8.45 $\pm$ 0.58 hr (Figure 7). Therefore, the CC population seems to rotate slower, but one has to keep in mind the large error bar in the mean rotational period because of the still limited sample. On the basis of Figure 7 and Tables 2 and 4, one can appreciate that most of the partial light curves have been obtained over 5–6 hr. As the typical TNO mean rotational period is about 8 hr, most of these partial light curves should have covered almost the full object's rotation, and, thus, a rough period estimate should have been estimated.

An important parameter to take into account is the size range of the CCs and the other TNOs. The CCs observed for light-curve studies have an absolute magnitude between 5 and 11.7 mag, whereas the other TNOs belong to the size range of −1.1 up to 9.8 mag. Therefore, both samples have overlap, but one has to keep in mind that the other TNOs sample has dwarf planets and large/medium-sized TNOs that are not present in the CC population. Also, there are only two very small CCs with $H > 10$ mag observed for light curves. Therefore, the two samples are mostly overlapping in the range of 5–9 mag. In Figure 8, we plotted all the TNOs from our sample and the literature with a partial, flat, or a full light curve. On the basis of the running means in Figure 8, the CC population tends to have more amplitude at small sizes, whereas the other TNOs have roughly a flat distribution across size ranges. In the case of the CC population, there is a constant increase of amplitude starting at $H \sim 6$ mag. The last bins ($H > 9$ mag) only have zero or one object per bin, and so the running mean is not adequate. In conclusion, it seems that the CC population is showing more light-curve variability than the other TNOs (Figure 9). We also checked for any trend between rotational period and size but did not find any relation. The CC population may also have slower rotations. As these properties are not noticed in the other TNO sample, we infer that they are primordial characteristics (Figure 9). More complete light curves of CCs and other TNOs, and especially small objects, would help to confirm these results. Also, the slower rotation of the CCs can be due to the loss of wide binaries satellites through the conservation of angular momentum, assuming that most of the CCs were born as binaries.

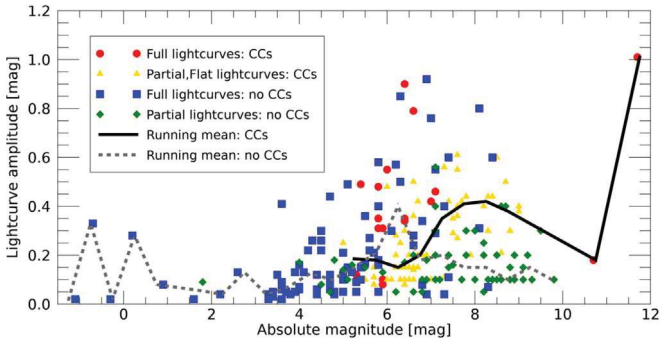

Figure 8. We used our results and the literature to plot the light-curve amplitude versus absolute magnitude distributions of the CC population and of the other TNOs. Different symbols and colors are used to separate the two populations and the partial/full light-curve sample. Two running means using the partial and the full light curves are overplotted, one for the CC population and one for the other TNOs. The other TNOs have a roughly flat distribution across the different size regimes, whereas the CC population is showing an increase of amplitude at small sizes. Some bins only have one or zero object.

4.3. Anticorrelation/Correlation

One can investigate trends between rotational properties and orbital elements for the CC population with the Spearman rank correlation (Spearman 1904). We calculated the Spearman coefficient (ρ) and the significance level (SL). A correlation is strong if $|\rho| > 0.6$, weak if $|\rho| > 0.3$, and nonexistent if $|\rho| < 0.3$. The SL is very strong if >99%, strong if >97.5%, and reasonably strong if >95%.

In a first step, we considered only the full light curves from the literature and our sample. Sila–Nunam is likely tidally locked and will not be considered in our search for correlations with rotational period but will be considered for light-curve amplitude (Rabinowitz et al. 2014). Our results are summarized in Table 5, and we emphasize that the sample of objects with a full light curve is limited to 16 CCs (with Sila–Nunam). There is a correlation between light-curve amplitude and rotational period, suggesting that the slow rotators tend to have larger light-curve amplitudes (i.e., objects more deformed or irregular shape). Such a tendency is confirmed by taking into account only the known resolved binaries and the potential contact binaries. As the samples are still limited, it is unclear whether we are dealing with an observational bias. If true, and because the sample is dominated by binaries, this correlation may give us some clues about binary system formation (Thirouin et al. 2014). Also, such a tendency is not observed in the rest of the trans-Neptunian belt.

The correlation search can also be performed using lower/upper limits, as implemented in the astronomy survival analysis package named ASURV[5] (Spearman 1904; Feigelson & Nelson 1985; Isobe et al. 1986; Isobe & Feigelson 1990; Lavalley et al. 1990, 1992). Therefore, our second step was for statistical tests in our merged sample of full and partial light curves (Table 5). Flat light curves reported here were not used for the correlation search. We noticed a weak correlation between light-curve amplitude and absolute magnitude (i.e., smaller objects have larger amplitude). Such a tendency has been already reported in several dynamical subpopulations, as well as in the entire TNO population, and is in agreement with

[5] http://astrostatistics.psu.edu/statcodes/asurv

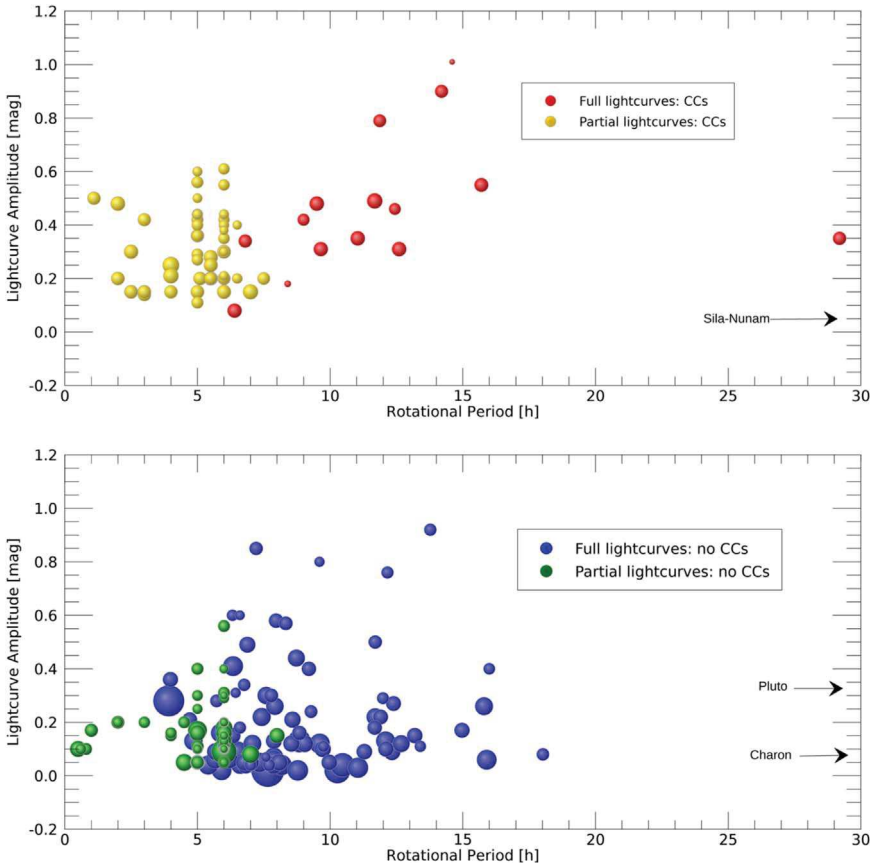

Figure 9. Upper panel summarizes the light-curve studies for the CC population, and the lower one is for the other TNOs. The bubble size indicates the size of the objects (i.e., large bubbles for large objects). The largest visible bubble is for Makemake ($H = -0.3$ mag, periodicity of 7.65 hr). The same bubble scaling has been used for both plots, allowing a direct comparison between theses two populations. Because of their very long rotational periods (out of the plot's scale), Sila–Nunam and Pluto-Charon are not plotted.

the TNO collisional evolution (Davis & Farinella 1997; Sheppard et al. 2008; Duffard et al. 2009; Benecchi & Sheppard 2013; Thirouin 2013; Alexandersen et al. 2018).

In a third step, we divided our sample according to absolute magnitude: (i) CCs with $H \leqslant 6$ mag (i.e., "large" objects, sample dominated by resolved binaries), (ii) CCs with $6 < H \leqslant 8$ mag (i.e., "medium-sized" objects, sample presumably dominated by single objects and unresolved binaries), and (iii) CCs with $8 < H \leqslant 12$ mag (i.e., "small" objects, sample likely dominated by single objects). The large objects sample shows a potential anticorrelation between period and eccentricity with a low SL. The medium-sized sample shows a weak anticorrelation between period and absolute magnitude, suggesting that the large objects rotate slower. A possible explanation is that the binaries dominate at large sizes and they undergo tidal effects able to slow down their rotations (Thirouin et al. 2014). Also, it is important to point out that the potential contact binaries are in this size range and that the cutoff at $H = 6$ mag to infer whether an object is perhaps a resolved binary is only approximate (Noll et al. 2014). There is a weak correlation between rotational period and absolute magnitude, with a SL of only 81%. Such a tendency, if true, is interesting, as the medium-sized objects display the opposite relation. The sample composed of the smallest objects presents a reasonably strong anticorrelation between rotational period and semimajor axis. Also, there are several trends with SLs below our threshold of confidence. For example, there is a weak anticorrelation between amplitude and eccentricity, indicating that large-amplitude CCs have low eccentricities. It is unclear whether such tendencies are an observational bias, as the sample at small size is still limited.

5. Contact Binaries

5.1. Definition

The definition of contact binary systems includes objects with a peanut shape or bilobed shape (like comet 67P), two objects touching in one point and thus in contact, and two objects with a small separation. To confirm the nature of the system/object, multiple light curves obtained at several epochs are required for modeling purposes. Also, multichord stellar occultations or even flybys can infer the shape (e.g., 2014 MU_{69}, Moore et al. 2018). Therefore, we adopted the following definition: (i) a light curve with an inverted-U shape at the maximum of brightness, a V shape at the minimum, and a peak-to-peak amplitude greater than 0.9 mag[6] is due to a *confirmed* contact binary (Dunlap & Gehrels 1969; Leone et al. 1984; Cellino et al. 1985; Sheppard & Jewitt 2004; Lacerda 2011; Lacerda et al. 2014); and (ii) a light curve with an inverted-U shape at the maximum of brightness, a V shape at the minimum, and a large peak-to-peak amplitude but not reaching the 0.9 mag threshold is due to a *likely* contact binary (Lacerda et al. 2014; Thirouin et al. 2017; Thirouin & Sheppard 2017, 2018). The morphology of a

[6] An object in hydrostatic equilibrium with a light-curve amplitude greater than 0.9 mag will break and create a binary (Weidenschilling 1980; Leone et al. 1984).

Table 5
Summary of Our Search for Correlation/Anticorrelation Using Semimajor Axis (a), Eccentricity (e), Inclination (i), Perihelion Distance (q), and Aphelion Distance (Q) from the Minor Planet Center (2018 November)

Correlated Values	Sample	ρ	SL (%)	Nb
Full light curves				
Δm versus P	with Sila	0.358	84	16
Δm versus P[a]	no Sila	0.596	98	15
Δm versus P	Binaries[b]	0.651	95	10
Δm versus i	with Sila	−0.126	38	16
Δm versus i	no Sila	−0.151	43	15
Δm versus i	Binaries	0.061	16	10
Δm versus e	with Sila	−0.090	29	16
Δm versus e	no Sila	−0.285	72	15
Δm versus e	Binaries	0.224	55	10
Δm versus a	with Sila	−0.099	31	16
Δm versus a	no Sila	−0.108	32	15
Δm versus a	Binaries	−0.073	19	10
Δm versus H	with Sila	0.335	81	16
Δm versus H	no Sila	0.212	58	15
Δm versus H	Binaries	0.556	91	10
Δm versus q	with Sila	0.088	28	16
Δm versus q	no Sila	0.275	71	15
Δm versus q	Binaries	−0.191	48	10
Δm versus Q	with Sila	−0.115	35	16
Δm versus Q	no Sila	−0.240	64	15
Δm versus Q	Binaries	0.159	40	10
P versus e	with Sila	−0.256	68	16
P versus e	no Sila	−0.097	28	15
P versus e	Binaries	−0.360	72	10
P versus i	with Sila	−0.101	30	16
P versus i	no Sila	−0.079	23	15
P versus i	Binaries	−0.140	33	10
P versus a	with Sila	0.135	40	16
P versus a	no Sila	0.175	49	15
P versus a	Binaries	−0.152	35	10
P versus H	with Sila	−0.093	28	16
P versus H	no Sila	0.103	30	15
P versus H	Binaries	−0.147	34	10
P versus q	with Sila	0.339	81	16
P versus q	no Sila	0.197	54	15
P versus q	Binaries	0.396	77	10
P versus Q	with Sila	−0.094	28	16
P versus Q	no Sila	0.047	14	15
P versus Q	Binaries	−0.311	65	10
Full+partial light curves				
Δm versus P	All, with Sila	−0.076	45	64
Δm versus P	All, no Sila	−0.047	29	63
Δm versus P	$H \leqslant 6$, no Sila	0.142	35	11
Δm versus P	$H \leqslant 6$, with Sila	−0.089	23	12
Δm versus P	$6 < H \leqslant 8$	0.051	25	41
Δm versus P	$8 < H \leqslant 12$	0.056	15	13
Δm versus i	All	−0.194	88	64
Δm versus i	$H \leqslant 6$	−0.087	23	12
Δm versus i	$6 < H \leqslant 8$	−0.270	91	41
Δm versus i	$8 < H \leqslant 12$	−0.408	80	11
Δm versus e	All	0.062	38	64
Δm versus e	$H \leqslant 6$	0.129	33	12
Δm versus e	$6 < H \leqslant 8$	0.022	11	41
Δm versus e	$8 < H \leqslant 12$	−0.472	86	11
Δm versus a	All	0.005	3	64
Δm versus a	$H \leqslant 6$	0.100	26	12
Δm versus a	$6 < H \leqslant 8$	−0.040	20	41
Δm versus a	$8 < H \leqslant 12$	−0.135	33	11
Δm versus H	All	0.273	97	64
Δm versus H	$H \leqslant 6$	0.186	46	12
Δm versus H	$6 < H \leqslant 8$	0.186	76	41
Δm versus H	$8 < H \leqslant 12$	0.068	17	11
Δm versus q	All	−0.042	26	64
Δm versus q	$H \leqslant 6$	0.020	5	12
Δm versus q	$6 < H \leqslant 8$	−0.026	13	41
Δm versus q	$8 < H \leqslant 12$	0.472	86	11
Δm versus Q	All	0.040	25	64
Δm versus Q	$H \leqslant 6$	0.230	55	12
Δm versus Q	$6 < H \leqslant 8$	0.001	1	41
Δm versus Q	$8 < H \leqslant 12$	−0.472	86	11
P versus e	All, with Sila	−0.270	97	64
P versus e	All, no Sila	−0.207	90	63
P versus e	$H \leqslant 6$, with Sila	−0.449	86	12
P versus e	$H \leqslant 6$, no Sila	−0.191	45	11
P versus e	$6 < H \leqslant 8$	−0.075	37	41
P versus e	$8 < H \leqslant 12$	−0.342	72	11
P versus i	All, with Sila	−0.045	28	64
P versus i	All, no Sila	−0.047	29	63
P versus i	$H \leqslant 6$, with Sila	−0.087	23	12
P versus i	$H \leqslant 6$, no Sila	−0.121	30	11
P versus i	$6 < H \leqslant 8$	0.203	80	41
P versus i	$8 < H \leqslant 12$	−0.444	84	11
P versus a	All, with Sila	−0.200	89	64
P versus a	All, no Sila	−0.183	85	63
P versus a	$H \leqslant 6$, with Sila	−0.181	45	12
P versus a	$H \leqslant 6$, no Sila	−0.087	22	11
P versus a	$6 < H \leqslant 8$	−0.147	65	41
P versus a	$8 < H \leqslant 12$	−0.611	95	11
P versus H	All, with Sila	−0.410	99	64
P versus H	All, no Sila	−0.364	99	63
P versus H	$H \leqslant 6$, with Sila	−0.252	60	12
P versus H	$H \leqslant 6$, no Sila	0.018	5	11
P versus H	$6 < H \leqslant 8$	−0.375	98	41
P versus H	$8 < H \leqslant 12$	0.417	81	11
P versus q	All, with Sila	0.138	73	64
P versus q	All, no Sila	0.071	42	63
P versus q	$H \leqslant 6$, with Sila	0.435	85	12
P versus q	$H \leqslant 6$, no Sila	0.210	49	11
P versus q	$6 < H \leqslant 8$	−0.076	37	41
P versus q	$8 < H \leqslant 12$	0.073	18	11
P versus Q	All, with Sila	−0.255	97	64
P versus Q	All, no Sila	−0.204	89	63
P versus Q	$H \leqslant 6$, with Sila	−0.313	70	12
P versus Q	$H \leqslant 6$, no Sila	−0.110	27	11
P versus Q	$6 < H \leqslant 8$	−0.115	53	41
P versus Q	$8 < H \leqslant 12$	−0.489	88	11

Notes. Sila–Nunam is excluded/included in our samples as it is a tidally locked system. Two OSSOS objects are not fully characterized yet, and so they are not included in our search with orbital elements, but they are included in the samples for the Δm versus P.
[a] Without Sila-Nunam and 2002 GV_{31}, $\rho = 0.718$ and SL = 99%.
[b] Contact and resolved binaries.

contact binary light curve can be produce by objects with other shapes, as suggested by Zappala (1980) and Harris & Warner (2018). Thus, it is also important to take into consideration the likelihood of such options. Finally, we want to point out that the recent flyby of 2014 MU_{69} clearly demonstrated the

existence of contact binaries in the trans-Neptunian belt (Stern et al. 2019).

5.2. Current Status in the CC Population

In about 1 year, the number of confirmed/likely contact binaries in the trans-Neptunian belt grew from two to nine (Sheppard & Jewitt 2004; Lacerda et al. 2014; Thirouin et al. 2017; Thirouin & Sheppard 2017, 2018, and this work). Thirouin & Sheppard (2018) showed an abundance of Plutino contact binaries. Thirouin & Sheppard (2017) and this work highlight the discovery of two likely contact binaries in the CC population, 2002 CC_{249} and 2004 VC_{131}, and have hints that 2004 VU_{75} and 2004 MU_8 are good candidates for this category.

Using the formalism from Sheppard & Jewitt (2004), we estimate the equal-sized contact binary fraction in the CC population. In case of an object with axes as $a > b$ and $b = c$, the light-curve amplitude changes with the angle of the object's pole relative to the perpendicular of the line sight (θ):

$$\Delta_m = 2.5 \log\left(\frac{1 + \tan\theta}{(b/a) + \tan\theta}\right). \quad (1)$$

The light-curve amplitude of an ellipsoid ($a \geqslant b = c$) varies as:

$$\Delta_m = 2.5 \log\left(\frac{a}{b}\right) - 1.25 \log\left[\left(\left(\frac{a}{b}\right)^2 - 1\right)\sin^2\theta + 1\right]. \quad (2)$$

Pole orientation aspects are important to estimate the fraction of contact binaries, and, thus, we will consider several cases. An object with $a/b = 3$ will display a variability of 0.9 mag if $\theta = 10°$. The probability of observing an object from a random distribution within 10° of the sight line is $P(\theta \leqslant 10°) = 0.17$. Similarly, and as discussed in Thirouin & Sheppard (2018), we can estimate the probability of different θ angles using different cutoffs for the amplitudes,[7] and therefore debias the pole orientations of our objects. As mentioned, the large amplitude is reached only when the system's components are equator-on. Therefore, considering smaller amplitude for an equator-off configuration is needed.

Using previous equations and several cutoffs for the light-curve amplitude (and so different $P(\theta)$), we estimate the contact binary fraction on the basis of our sample[8] and assuming equal-sized binaries. We found that $f(\Delta m \geqslant 0.7\,\mathrm{mag}) \sim 1/(42 \times P(\theta \leqslant 20°)) \sim 7\%$, and $f(\Delta m \geqslant 0.5\,\mathrm{mag}) \sim 8\%$ using Equation (1). On the basis of Equation (2), we estimated for our sample $f(\Delta m \geqslant 0.7\,\mathrm{mag}) \sim 6\%$ and $f(\Delta m \geqslant 0.5\,\mathrm{mag}) \sim 8\%$. Potential contact binaries reported here have an absolute magnitude ranging from 6 to 7 mag, and only taking into account objects in this size range, we found $f(\Delta m \geqslant 0.5\,\mathrm{mag}; 6 \leqslant H \leqslant 7) \sim 9\%$ and $f(\Delta m \geqslant 0.5\,\mathrm{mag}; 6 \leqslant H \leqslant 7) \sim 10\%$ with Equation (1) and Equation (2), respectively. In conclusion, the contact binary fraction in the CC population is less, or about 10% on the basis of our entire sample and a specific size range. Using our data set and the literature, we calculated[9] $f(\Delta m \geqslant 0.7\,\mathrm{mag}) \sim 7\%$ and $f(\Delta m \geqslant 0.7\,\mathrm{mag}) \sim 6\%$ with Equation (1) and Equation (2), respectively. Assuming a cutoff[10] at 0.5 mag, we obtained with both equations the same result $f(\Delta m \geqslant 0.5\,\mathrm{mag}) \sim 15\%$.

Despite the hints that 2004 VU_{75} and 2004 MU_8 are perhaps contact binaries, we did not include them in our previous estimates as we do not have their full light curves (and, thus, a secure light-curve amplitude estimate). However, as both objects have an amplitude larger than 0.4 mag in a few hours, we can assume that their full light curves will likely be larger than 0.5 mag and we can include them in our $f(\Delta m \geqslant 0.5\,\mathrm{mag})$ estimate. For our sample only, we obtained $f(\Delta m \geqslant 0.5\,\mathrm{mag}) = 16\%$ and 17% with Equation (1) and Equation (2), respectively. With our sample and the literature, the fraction is the same for both equations, $f(\Delta m \geqslant 0.5\,\mathrm{mag}) = 19\%$. Two objects from Alexandersen et al. (2018) are good candidates for follow-up observations on the basis of their potential large amplitude, 2015 RO_{281} and 2013 UL_{15}. Assuming that these objects have a full amplitude larger than 0.4 mag, we estimated that $f(\Delta m \geqslant 0.4\,\mathrm{mag}) = 21\%$ and 25% with Equation (1) and Equation (2), respectively. Other objects have $\Delta m > 0.4$ mag, but as their light curves are noisy, they are not considered in our previous estimates. Finally, we emphasize that these fractions are lower limits, and more full light curves are required for several objects in order to infer their shape as well as continue to build a representative sample of the CC population. Also, we are only considering near equal-sized binaries for our estimate, and, thus, the fraction will increase by adding the nonequal-sized binaries. For the purpose of this section, we assumed that none of the flat light curves is due to contact binaries with a pole-on orientation. Contact binaries with very long rotational periods undetectable over our observing blocks are not considered. Therefore, as already said, the previous percentages are lower limits.

5.3. CCs versus Plutinos

The contact binary population in the Kuiper Belt has been estimated to up to 30% (Sheppard & Jewitt 2004; Lacerda et al. 2014). However, we find that only 10%–25% of the CCs are likely near equal-sized contact binaries. Therefore, it seems that there is a deficit of contact binaries in the CC population. On the other hand, with the same type of observations and analysis, we found an excess of near equal-sized contact binaries with an estimate up to 40%–50% in the Plutino population (Thirouin & Sheppard 2018). Such a find (despite the still low statistical number) is interesting, especially because the opposite tendency is noticed with the resolved wide binaries: a deficit of resolved wide binaries in the Plutinos and an excess in the CC population (Noll et al. 2008a; Thirouin & Sheppard 2018). Also, it is interesting to mention that the size of the likely contact binaries found in these two subpopulations is different. In the Plutino population, the likely contact binaries have an absolute magnitude around 7 mag, whereas they are larger with an absolute magnitude around 6 mag in the CC group (Figure 10, except for the potential contact binary 2004 VU_{75} with $H = 6.7$ mag). For both studies, we used the same observing strategy for partial/full light curve, and we also focused on a large range of objects' sizes, allowing a comparison of these two subpopulations (Figure 10). However, as the CCs are further away compared to the Plutinos, we have

[7] An amplitude of 0.4/0.5/0.6/0.7 mag is for $\theta = 49°/36°/27°/20°$.

[8] Despite its large amplitude, the known resolved binary Logos–Zoe is not taken into account in our estimates as a contact binary.

[9] We considered that only two CCs have a light-curve amplitude >0.7 mag: 2002 CC_{249} and 2003 BF_{91}. Kern & Elliot (2006) reported an amplitude 0.90 ± 0.36 mag for the satellite of 2003 QY_{90}, but on the basis of their very sparse light curve and large uncertainty, we have not taken into account this object.

[10] Seven CCs have a light-curve amplitude >0.5 mag, 2002 CC_{249}, 2003 BF_{91}, 2004 VC_{131}, 2013 SM_{100}, 2013 UN_{13}, 2015 RA_{280}, and 2015 RB_{280}. We did not take into account uo3l88 because the light curve presents a large dispersion.

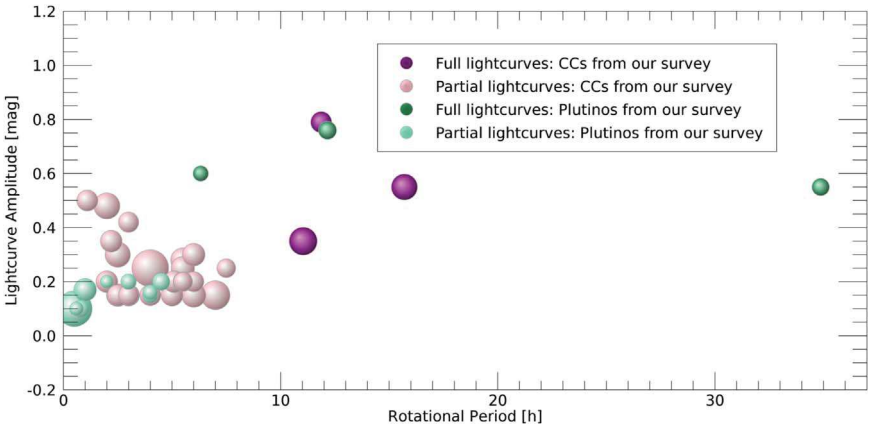

Figure 10. Partial/full light curves obtained with our surveys of the CC and Plutino populations. The potential Plutino contact binaries are smaller than the ones found in the CC population. We observed a handful of Plutinos compared to the CCs and found an abundance of contact binaries.

the tendency to observe larger CCs on average. So, observing smaller fainter CCs may find more contact binaries, as in the Plutino population. One possible explanation for the contact binary fractions is linked to the formation/evolution of these two populations. As said, the CC population was likely formed in situ and never suffered any strong dynamical evolution, whereas the resonance populations have not been formed where they are today and have been pushed outward during the migration of Neptune. Therefore, the formation/evolution of theses two subpopulations is different. Assuming that all planetesimals formed as binary systems, the different fractions of contact binaries are likely an outcome of the higher velocity dispersion and more intense and longer dynamical interactions that the resonance populations likely encountered after formation (Nesvorný et al. 2018). To confirm such a find, more contact binaries have to be found, and we also need to test other resonances to infer whether the high-contact binary fraction is present in all resonances or only the 3:2.

6. Context for New Horizons: (486958) 2014 MU_{69}

The second target of the *NASA New Horizons* spacecraft is a small CC TNO with an absolute magnitude $H = 11.1$ mag. Only two CCs in this size range have been observed for light-curve variability, 2003 BF_{91} and 2003 BG_{91}, and thus can be used as comparison for 2014 MU_{69}. Both have slow rotations with periods of 8.4 and 14.6 hr, and 2003 BF_{91} displays a large amplitude of about 1 mag, whereas 2003 BG_{91} has a moderate amplitude of 0.18 mag. Both light curves have been obtained with the *HST* and present a large dispersion, and binning was needed to produce the light curves. Unfortunately, both objects have not been observed since 2003 (orbital arcs of 13 and 92 days) and, thus, are likely lost. Despite the very limited sample of very small CCs to which we can compare 2014 MU_{69}, we can use the rest of the CC population for extrapolation. In fact, by observing a large number of CCs over diverse size range, we can infer the rotational and physical properties of this population and extrapolate to smaller sizes. So far, we have shown that the CCs tend to rotate slowly and are more deformed than the other TNOs. Also, there is an increase of light-curve amplitude with decreasing size, suggesting that the small CCs are more deformed than the large ones. If 2014 MU_{69} follows similar trends, we have to expect a slow rotator with a deformed shape. Results from a stellar occultation by 2014 MU_{69} seems to indicate that the shape is complex and, thus, confirms our trend. However, on the basis of *HST* data, it seems that the light curve of 2014 MU_{69} is flat (Benecchi et al. 2017, 2018). A reasonable explanation to reconcile the occultation and light-curve data is to consider that 2014 MU_{69} has a (nearly) pole-on orientation, which was confirmed by the flyby (Showalter et al. 2019; Zangari et al. 2019). On the basis of the preliminary results from the flyby, 2014 MU_{69} has a potential rotational period of 15 ± 1 hr (Stern et al. 2019). Therefore, 2014 MU_{69} seems to follow all the trends reported in this work.

On the basis of a stellar occultation and the flyby results, 2014 MU_{69} is a contact binary. In this work and Thirouin & Sheppard (2017), we report the discovery of two likely contact binaries and some hints for two more in the CC population. By taking into account our sample and the literature, we estimate that 10%–25% of the CC population could be contact binaries, suggesting that 2014 MU_{69} is one of the few CC contact binaries. So far, the likely CC contact binaries are "large" ($H \sim 6$ mag, except for 2004 VU_{75}), and, thus, it is interesting that we are not finding smaller CCs to be contact binaries as in the 3:2 population. However, we should also consider that the shape of these systems can be different with size: contact binaries with two separated or in-contact objects at large sizes and a peanut shape at smaller sizes.

7. Summary and Conclusions

Over the past 3 years, we used the DCT and the Magellan-Baade telescope to study the rotational properties of the dynamically CC TNOs. On the basis of our 42 complete/partial light curves and the literature, we derived information about the shape and the rotational period distributions of the CC population. Our results are as follows:

1. Our first results from our survey dedicated to the rotational and physical properties of the CC population are presented. This survey is the first one entirely dedicated to this subpopulation of the trans-Neptunian belt and provides context for the second flyby of the *NASA New Horizons* mission.
2. We report the discovery of one new likely contact binary in the CC population, 2004 VC_{131}, and we have evidence that 2004 MU_8 and 2004 VU_{75} are also perhaps contact binaries. We estimate that the CC population has only 10%–25% of near equal-sized contact binaries, compared

to the 40%–50% found in the 3:2 resonance (Thirouin & Sheppard 2018). This estimate is a lower limit and assumes near equal-sized binaries (Sheppard & Jewitt 2004). The likely fraction of contact binaries in both populations will increase if we also consider nonequal-sized contact binary systems.

3. Objects in the CC population display a larger variability than the other TNOs, suggesting that they are more elongated or deformed than the rest of the trans-Neptunian population. About 65% of the other TNOs have an amplitude below 0.2 mag, but only 36% of the CCs have a low variability. We also noticed a higher amplitude at smaller sizes, which is not noticed in the other TNO sample. Because these tendencies are not present in the rest of the trans-Neptunian population, they are probably primordial characteristics of the CC population.
4. Similarly, the CCs seem to rotate slower than the other TNOs, with a mean rotational period of 9.48 ± 1.53 hr compared to the 8.45 ± 0.58 hr for the rest of the TNOs. Once again, this slow rotation can be a primordial characteristic of the CC population.
5. We performed a search for correlation/anticorrelation between rotational and physical parameters using the sparse and full light curves and by using several size ranges. We report a strong correlation between rotational period and light-curve amplitude in the CC group (not noticed in the rest of the TNOs). There is no clear explanation yet for this trend.
6. We also report the discovery of a new nearly equal-sized wide binary, 2014 LQ_{28}, with a magnitude difference of about 0.4 mag between the two components. With $H = 5.7$ mag, 2014 LQ_{28} follows the trend that all large CCs are resolved binaries (Noll et al. 2014).
7. Our survey also provides context for the second flyby of the New Horizons mission. On the basis of early results, 2014 MU_{69} is a contact binary with a potential rotational period of about 15–16 hr (Stern et al. 2019). Therefore, 2014 MU_{69} is a slow rotator like the rest of the population. The shape of 2014 MU_{69} is not unusual in the trans-Neptunian belt as we already found several confirmed/likely contact binaries through their light curves. However, we do not find a lot of contact binaries in the CC group.

We thank the referee for her/his careful reading of this paper and useful comments. We also thank Larry Wasserman and Nuno Peixinho for their help with ASURV. We also acknowledge Chad Trujillo for some images obtained with the Lowell's Discovery Channel Telescope. Thanks go to M. Bannister and J.-M. Petit for the official designation of the OSSOS objects. This paper includes data gathered with the 6.5 m Magellan-Baade Telescope located at Las Campanas Observatory, Chile. This research is based on data obtained at the Lowell Observatory's Discovery Channel Telescope (DCT). Lowell is a private, nonprofit institution dedicated to astrophysical research and public appreciation of astronomy and operates the DCT in partnership with Boston University, the University of Maryland, the University of Toledo, Northern Arizona University, and Yale University. Partial support of the DCT was provided by Discovery Communications. LMI was built by Lowell Observatory using funds from the National Science Foundation (grant No. AST-1005313). The authors acknowledge the DCT and Magellan staffs. The authors also acknowledge support from the National Science Foundation (NSF), grant No. AST-1734484 awarded to the "Comprehensive Study of the Most Pristine Objects Known in the Outer Solar System."

Facilities: Lowell's Discovery Channel Telescope, Magellan-Baade telescope.

Software: ASURV (Isobe et al. 1986; Isobe & Feigelson 1990; Lavalley et al. 1990, 1992).

ORCID iDs

Audrey Thirouin https://orcid.org/0000-0002-1506-4248
Scott S. Sheppard https://orcid.org/0000-0003-3145-8682

References

Alexandersen, M., Benecchi, S. D., Chen, Y.-T., et al. 2018, ApJS, in press (arXiv:1812.04304)
Batygin, K., Brown, M. E., & Fraser, W. C. 2011, ApJ, 738, 13
Benecchi, S., Porter, S., Spencer, J., et al. 2018, arXiv:1812.04758
Benecchi, S. D., Buie, M. W., Porter, S. B., et al. 2017, AAS/DPS Meeting Abstracts, 49, 504.07
Benecchi, S. D., Noll, K. S., Grundy, W. M., et al. 2009, Icar, 200, 292
Benecchi, S. D., & Sheppard, S. S. 2013, AJ, 145, 124
Cellino, A., Pannunzio, R., Zappala, V., Farinella, P., & Paolicchi, P. 1985, A&A, 144, 355
Chandrasekhar, S. 1987, Ellipsoidal Figures of Equilibrium (New York: Dover)
Collander-Brown, S. J., Fitzsimmons, A., Fletcher, E., Irwin, M. J., & Williams, I. P. 1999, MNRAS, 308, 588
Davis, D. R., & Farinella, P. 1997, Icar, 125, 50
Duffard, R., Ortiz, J. L., Thirouin, A., Santos-Sanz, P., & Morales, N. 2009, A&A, 505, 1283
Dunlap, J. L., & Gehrels, T. 1969, AJ, 74, 796
Feigelson, E. D., & Nelson, P. I. 1985, ApJ, 293, 192
Gladman, B., Marsden, B. G., & Vanlaerhoven, C. 2008, in The Solar System Beyond Neptune, ed. M. A. Barucci, D. P. Cruikshank, & A. Morbidelli (Tucson, AZ: Univ. Arizona Press), 43
Grundy, W. M., Benecchi, S. D., Rabinowitz, D. L., et al. 2012, Icar, 220, 74
Grundy, W. M., Noll, K. S., Nimmo, F., et al. 2011, Icar, 213, 678
Harris, A. W., & Warner, B. 2018, AAS/DPS Meeting Abstracts, 50, 414.03
Howell, S. B. 1989, PASP, 101, 616
Isobe, T., & Feigelson, E. D. 1990, BAAS, 22, 917
Isobe, T., Feigelson, E. D., & Nelson, P. I. 1986, ApJ, 306, 490
Jeans, J. H. 1919, Problems of Cosmogony and Stellar Dynamics (Cambridge: Cambridge Univ. Press)
Kern, S. D. 2006, PhD thesis, MIT
Kern, S. D., & Elliot, J. L. 2006, Icar, 183, 179
Lacerda, P. 2011, AJ, 142, 90
Lacerda, P., & Luu, J. 2006, AJ, 131, 2314
Lacerda, P., McNeill, A., & Peixinho, N. 2014, MNRAS, 437, 3824
Lavalley, M. P., Isobe, T., & Feigelson, E. D. 1990, BAAS, 22, 917
Lavalley, M. P., Isobe, T., & Feigelson, E. D. 1992, BAAS, 24, 839
Leone, G., Paolicchi, P., Farinella, P., & Zappala, V. 1984, A&A, 140, 265
Levine, S. E., Bida, T. A., Chylek, T., et al. 2012, Proc. SPIE, 8444, 844419
Lomb, N. R. 1976, Ap&SS, 39, 447
Moore, J. M., McKinnon, W. B., Cruikshank, D. P., et al. 2018, GeoRL, 45, 8111
Nesvorný, D., Parker, J., & Vokrouhlický, D. 2018, AJ, 155, 246
Noll, K. S., Grundy, W. M., Chiang, E. I., Margot, J.-L., & Kern, S. D. 2008a, in The Solar System Beyond Neptune, ed. M. A. Barucci, D. P. Cruikshank, & A. Morbidelli (Tucson, AZ: Univ. Arizona Press), 345
Noll, K. S., Grundy, W. M., Stephens, D. C., Levison, H. F., & Kern, S. D. 2008b, Icar, 194, 758
Noll, K. S., Parker, A. H., & Grundy, W. M. 2014, AAS/DPS Meeting Abstracts, 46, 507.05
Noll, K. S., Stephens, D. C., Grundy, W. M., et al. 2002, AJ, 124, 3424
Noll, K. S., Stephens, D. C., Grundy, W. M., Osip, D. J., & Griffin, I. 2004, AJ, 128, 2547

Osip, D. J., Kern, S. D., & Elliot, J. L. 2003, EM&P, 92, 409
Pál, A., Szabó, R., Szabó, G. M., et al. 2015, ApJL, 804, L45
Peixinho, N., Lacerda, P., & Jewitt, D. 2008, AJ, 136, 1837
Penteado, P. F., Trilling, D. E., & Grundy, W. 2016, AAS/DPS Meeting Abstracts, 48, 120.20
Pike, R. E., Fraser, W. C., Schwamb, M. E., et al. 2017, AJ, 154, 101
Rabinowitz, D. L., Benecchi, S. D., Grundy, W. M., & Verbiscer, A. J. 2014, Icar, 236, 72
Romanishin, W., & Tegler, S. C. 1999, Natur, 398, 129
Santos-Sanz, P., Ortiz, J. L., Barrera, L., & Boehnhardt, H. 2009, A&A, 494, 693
Sheppard, S. S., & Jewitt, D. 2004, AJ, 127, 3023
Sheppard, S. S., & Jewitt, D. C. 2002, AJ, 124, 1757
Sheppard, S. S., Lacerda, P., & Ortiz, J. L. 2008, in The Solar System Beyond Neptune, ed. M. A. Barucci, D. P. Cruikshank, & A. Morbidelli (Tucson, AZ: Univ. Arizona Press), 129
Sheppard, S. S., & Thirouin, A. 2018, CBET, 4483
Showalter, M. R., Buie, M. W., Grundy, W. M., et al. 2019, LPI, 50, 2132
Spearman, C. 1904, Am. J. Psychol., 15, 72
Stellingwerf, R. F. 1978, ApJ, 224, 953
Stephens, D. C., & Noll, K. S. 2006, AJ, 131, 1142
Stern, S. A., Spencer, J. R., Weaver, H. A., et al. 2019, arXiv:1901.02578
Stetson, P. B. 1987, PASP, 99, 191
Thirouin, A. 2013, PhD thesis, Univ. Granada
Thirouin, A., Noll, K. S., Ortiz, J. L., & Morales, N. 2014, A&A, 569, A3
Thirouin, A., Ortiz, J. L., Campo-Bagatin, A., et al. 2012, MNRAS, 424, 3156
Thirouin, A., Ortiz, J. L., Duffard, R., et al. 2010, A&A, 522, A93
Thirouin, A., & Sheppard, S. S. 2017, AJ, 154, 241
Thirouin, A., & Sheppard, S. S. 2018, AJ, 155, 248
Thirouin, A., Sheppard, S. S., & Noll, K. S. 2017, ApJ, 844, 135
Trilling, D. E., & Bernstein, G. M. 2006, AJ, 131, 1149
Weidenschilling, S. J. 1980, Icar, 44, 807
Zangari, A. M., Beddingfield, C. B., Benecchi, S. D., et al. 2019, LPI, 50, 3007
Zappala, V. 1980, M&P, 23, 345